

TEXTURAL AND GEOTHERMOMETRIC ASPECTS  
OF SODIUM DISTRIBUTION IN FELDSPARS  
FROM TWO AREAS IN THE GRENVILLE  
PROVINCE, QUEBEC

by

Nathan Arthur Camille Rey

A thesis submitted to the School of Graduate  
Studies in partial fulfillment of the requirements  
for the degree of M.Sc. in Geology

UNIVERSITY OF OTTAWA  
OTTAWA, CANADA, 1978

UMI Number: EC56168

### INFORMATION TO USERS

The quality of this reproduction is dependent upon the quality of the copy submitted. Broken or indistinct print, colored or poor quality illustrations and photographs, print bleed-through, substandard margins, and improper alignment can adversely affect reproduction.

In the unlikely event that the author did not send a complete manuscript and there are missing pages, these will be noted. Also, if unauthorized copyright material had to be removed, a note will indicate the deletion.

**UMI<sup>®</sup>**

---

UMI Microform EC56168  
Copyright 2011 by ProQuest LLC  
All rights reserved. This microform edition is protected against  
unauthorized copying under Title 17, United States Code.

---

ProQuest LLC  
789 East Eisenhower Parkway  
P.O. Box 1346  
Ann Arbor, MI 48106-1346

#### ACKNOWLEDGEMENTS

This project, proposed by Dr. J. Bourne of the Geological Survey of Canada, was researched and written under the supervision of Dr. R. Kretz.

Thanks are given to Dr. K. Currie, of the Geological Survey of Canada, whose editorial comments were incisive, and to Dr. A. J. Baer, whose interest in the project exceeded the call of duty.

## ABSTRACT

The plagioclase and perthitic alkali feldspars of twenty-seven samples from two field areas were intensively subjected to electron microprobe analysis for geothermometric purposes. Plagioclase analyses agree closely with results obtained from flat-stage optical determinations. The composition of plagioclase lamellae in alkali feldspar is always very similar to that of external plagioclase crystals, implying that exsolution of plagioclase from alkali feldspar occurred in equilibrium with external plagioclase. However, results indicate that the host phase of the alkali feldspar is not homogeneous. Furthermore, when the analysed feldspar compositions are applied to Stormer's (1975) geothermometer, the temperatures obtained are 100 to 150° below those of the inferred maximum metamorphic grade of the rocks.

Atomic absorption analysis of alkali feldspar isolated from selected samples indicates variability in bulk composition of the alkali feldspar. However, a modified immersion oil technique failed to corroborate inhomogeneity in the host phase of the alkali feldspar, owing to imprecision in the technique.

Petrographic investigation of selected samples revealed visible zones where exsolved plagioclase lamellae have been expelled from the alkali feldspar crystals. The expelled plagioclase precipitated on adjoining plagioclase crystals as myrmekitic oligoclase or as albite. This expulsion process, active under conditions of falling temperature, resulted in an inhomogeneous, sodium-poor host phase of the perthitic alkali feldspar.

TABLE OF CONTENTS

	Page
List of Illustrations	vii
List of Tables	viii
List of Plates	ix
Introduction	1
Feldspar Geothermometry	3
Field Areas and Regional Geology	16
Blue Sea Lake Area	16
Old Chelsea Outcrop	20
Electron Microprobe Analysis	27
Equipment and Technique	27
Standard Analyses	29
Analyses from Study Areas: Recalculation and Tabulation	32
Microprobe Data: Blue Sea Lake Area	40
Microprobe Data: Old Chelsea Outcrop	40
Discussion of Old Chelsea Outcrop Data	46
Discussion of Microprobe Data	46
Oil Immersion Study	54
Method Employed	54
Discussion of Method	60
Calibration of Method	62
Data	67

	Page
Atomic Absorption Spectroscopy	70
Method of Analysis	70
Data	71
Discussion of Data	73
Synthesis of Analytical Results	75
Petrography: Old Chelsea Outcrop	78
General Texture and Mineralogy	78
Classification of Rock Types in Old Chelsea Outcrop	81
General Texture	82
Descriptive Mineralogy	86
Alteration of the Old Chelsea Granodiorite	95
Exsolved Feldspar: Old Chelsea Outcrop	109
Alkali Feldspar Exsolved from Plagioclase	109
Plagioclase Exsolved from Alkali Feldspar	109
Discussion	127
Suggested Further Research	130
References	132

## LIST OF ILLUSTRATIONS

Figure		Page
1	Barth's (1951) Geothermometer	8
2	Stormer's (1975) Geothermometer	10
3	Location Map Of Blue Sea Lake Area	19
4	Location Map Of Old Chelsea Outcrop	21
5	Blue Sea Lake Sample Locations	42
6	Relative Positions Of Old Chelsea Outcrop Samples	45
7	Refringence Relationships Of A Sample Grain Of Microcline Mounted In Immersion Oil	56
8	Oil Immersion Study: Quartz Calibration Results	66
9	Bulk Felsic Mineralogy (After Streckeisen, 1967): Old Chelsea Suite	85
10	Correlation Of Albite Rims On Plagioclase To Nearby Alkali Feldspar	100
11	Correlation Of Albite Rims On Plagioclase To Degree Of Alteration	103
12	Loss Of Plagioclase From Alkali Feldspar Crystals	106
13	Correlations Of Exsolved Plagioclase In Alkali Feldspar To Modes of Alkali Feldspar	125

LIST OF TABLES

Table		Page
1	Reliability Of Standard Probe Analyses	31
2	Electron Microprobe Results: Normal Plagioclase And Alkali Feldspar	33
3	Electron Microprobe Results: Exsolved Plagioclase And Alkali Feldspar	39
4	Na In Plagioclase: Probe Vs. Optics	49
5	Results Of Oil Immersion Study: Alkali Feldspar Of Old Chelsea Outcrop	68
6	Results Of Atomic Absorption Spectroscopy: Alkali Feldspar Old Chelsea Outcrop	72
7	Old Chelsea Outcrop: Bulk Mineral Modes	79
8	Modes Of Exsolved Plagioclase In Alkali Feldspar: Old Chelsea	110
9	Old Chelsea Outcrop: Detailed Albite Modes	122

LIST OF PLATES

Plate	Page
1	135
2	136
3	137
4	138
5	139
6	140
7	141

## INTRODUCTION

In April, 1976, the writer undertook a test of Stormer's (1975) two-feldspar geothermometer on poly-metamorphosed rocks. The geothermometer had at this time been used successfully on unmetamorphosed igneous rocks (Stormer, 1975, 1976) and requires only the coexistence at equilibrium of plagioclase and alkali feldspar. It was hoped that this common mineral association could be proven to be a reliable indicator of maximum metamorphic temperature (pressure being estimated by other means), for its applications, both to field mapping and theoretical petrology, would be myriad.

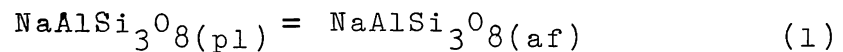
Originally it was intended that after some preliminary work, the geothermometer would ultimately be tested on rocks of varying grade ranging from lower amphibolite to upper granulite. In this way the metamorphic grades in which the geothermometer did and did not function efficiently were to be demarcated. Then the geothermometer was to be used on rocks of its "optimum" metamorphic grade to solve a theoretical problem. The preliminary testing, as discussed below, revealed these plans to be impossibly grandiose, and research was compelled towards projects of steadily

decreasing scale. However, despite the forced modifications in the objectives of this research, Stormer's two-feldspar geothermometer figures prominently in it. Therefore, a short discussion of the theory and history of feldspar geothermometry, and of Stormer's contributions to it, is relevant.

## FELDSPAR GEOTHERMOMETRY

The concept of feldspar geothermometry, utilizing the distribution of albite between the potash feldspar and plagioclase solid solutions, has a long and auspicious history. First proposed by Barth in 1934, it has since been extensively discussed and modified by Barth himself and by others (for a more complete discussion, see Stormer, 1975, p. 667). On the strength of modern thermodynamic data, Stormer (1975) has presented a workable two-feldspar geothermometer. Let us examine the improvements he has made, and the weaknesses which yet remain.

The partition of albite between plagioclase and potash feldspar is controlled by the following exchange reaction:



where the subscripts (pl) and (af) denote the host phases of the albite component, plagioclase and alkali feldspar, respectively. At equilibrium, thermodynamics requires that the chemical potential ( $\mu$ ) of the albite in both feldspars is equal:

$$\mu(\text{af}) = \mu(\text{pl}) \quad (2)$$

(3)

Notice that no solid or fluid phases besides the two feldspars participate in this equilibrium. Other phases may be present which may affect the concentration of sodium in the rock, but Stormer (1975) maintains that these other phases will not affect the equilibrium relationship of Equation (2).

The chemical potential of albite in each feldspar is related to activity which in turn is a function of composition:

$$a_{(af)} = X_{(af)} \gamma_{(af)} \quad (3)$$

$$a_{(pl)} = X_{(pl)} \gamma_{(pl)} \quad (4)$$

where  $a$  is the activity,  $X$  is the mole fraction, and  $\gamma$  is the activity coefficient, a correction factor for non-ideality in the plagioclase and alkali feldspar solid solutions. Now:

$$\mu_{(af)} = \mu'_{(af)} + RT \ln a_{(af)} \quad (5)$$

$$\mu_{(pl)} = \mu'_{(pl)} + RT \ln a_{(pl)} \quad (6)$$

where  $\mu'$  refers to the chemical potential of albite in any

convenient standard state.

Then from equations 2,5, and 6:

$$\mu'_{(pl)} - \mu'_{(af)} = RT \ln \frac{a_{(af)}}{a_{(pl)}} \quad (7)$$

Equation (7) can be taken to describe without assumptions the partition at equilibrium of albite between plagioclase and alkali feldspar (Stormer 1975).

Barth (1951) proposed a two-feldspar geothermometer using Equation (7), based on the assumption that the distribution of albite between the two host phases obeys the Nernst Distribution Law. If the Nernst Distribution Law is applied to the two-feldspar system, it requires that the solution of albite in plagioclase and alkali feldspar must follow equations (3) and (4) with  $\gamma$  independent of X, in accordance with Henry's Rule. If this is the case, the activity of albite in both solid solutions is directly proportional to concentration. This restriction does not require that  $\gamma_{(af)}$  and  $\gamma_{(pl)}$  both equal one, or even that they equal each other. It merely requires that the ratio  $\gamma_{(af)}/\gamma_{(pl)}$  does not vary with mole fraction.

Barth further assumed that the ratio  $\gamma_{(af)}/\gamma_{(pl)}$  does not vary with temperature, and if it is equally unaffected by mole fraction, then this ratio is equivalent to the ratio of activity coefficients for albite in any two convenient standard states:

$$\gamma_{(af)}/\gamma_{(pl)} = \gamma'_{(af)}/\gamma'_{(pl)}$$

Equation (7) could then be written:

$$\mu'_{(pl)} - \mu'_{(af)} = RT \ln \left( \frac{X_{(af)}}{X_{(pl)}} \cdot \frac{\gamma'_{(af)}}{\gamma'_{(pl)}} \right) \quad (8)$$

Expressing the ratio  $X_{(af)}/X_{(pl)}$  as the distribution coefficient  $K_D$ , Equation (8) becomes:

$$\ln K_D = \frac{\mu'_{(pl)} - \mu'_{(af)}}{RT} - \ln \frac{\gamma'_{(af)}}{\gamma'_{(pl)}} \quad (9)$$

Equation (9) is an expression of the Nernst Distribution Law. Now, since  $\gamma'_{(af)}/\gamma'_{(pl)}$  is assumed to be independent of temperature, Equation (9) becomes:

$$\ln K_D = \frac{a}{T} + b \quad (10)$$

where  $a = \mu'_{(pl)} - \mu'_{(af)}/R$  and  $b = -\ln \gamma'_{(af)}/\gamma'_{(pl)}$ .

Barth then empirically determined the coefficients a and b by calibrating his model against naturally occurring specimens whose temperatures of equilibration were roughly known. The resulting determinative curve is shown in Figure 1.

Ingenious though it was, Barth's (1951) rough-and-ready approximation had three flaws (Stormer, 1975): (1) The solution of albite in alkali feldspar deviates from Henry's Rule at many naturally occurring concentrations. (2) The geothermometer is only empirically calibrated; experimental data now exist. (3) Barth's approach did not consider the effect of pressure.

Stormer's (1975) geothermometer does not assume the above restrictions on the behavior of albite in alkali feldspar. Substituting equations (3) and (4) in Equation (7):

$$\mu'_{(pl)} - \mu'_{(af)} = RT \ln \frac{X_{(af)} \gamma_{(af)}}{X_{(pl)} \gamma_{(pl)}} \quad (11)$$

If pure albite is chosen as the standard state, the left-hand side of Equation (11) equals zero. Therefore:

$$X_{(pl)} \gamma_{(pl)} = X_{(af)} \gamma_{(af)} \quad (12)$$

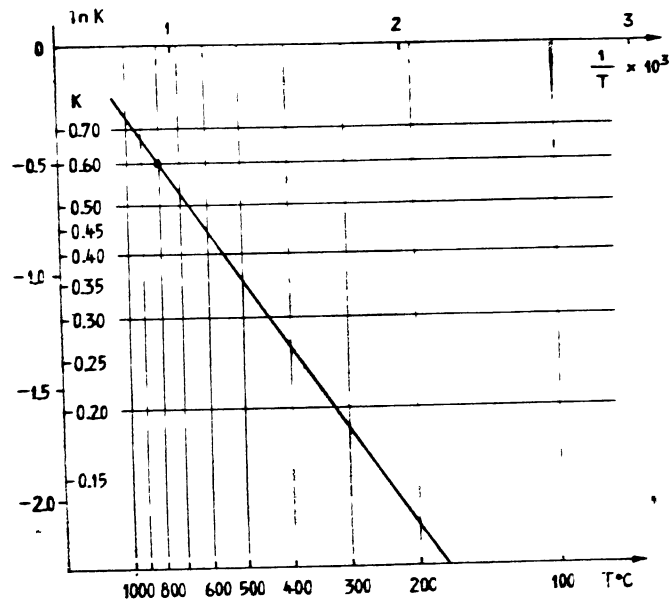


Figure 1: Barth's (1951) geothermometer.

$$K_D = \frac{X_{(af)}}{X_{(pl)}} = \frac{\gamma_{(pl)}}{\gamma_{(af)}} \quad (13)$$

At this point, Stormer assumes that "at the pressures and temperatures which are of most interest" albite dissolves nearly ideally in plagioclase. Then  $\gamma_{(pl)}$  would be unity and Equation (13) simplifies to:

$$K_D = \frac{1}{\gamma_{(af)}} \quad (14)$$

The assumption of albite dissolving ideally in plagioclase probably introduces little error, at least at moderately high temperatures. Analysis of solution properties of plagioclase (Saxena and Ribbe, 1972) using Orville's (1972) data indicates that the activity coefficient of plagioclase is nearly unity for compositions between  $Ab_{100}$  and  $Ab_{45}$  at 700 degrees Celsius. At higher temperatures, solidus curves calculated from standard enthalpy of fusion data, and assuming no deviation from Raoult's Law, show a maximum disparity of 15 ° C from experimental data (Bowen, 1913).

The thermodynamic expression of  $\gamma_{(af)}$  in terms of pressure and temperature is the crux of Stormer's geothermometer. Several sets of experimental data exist to choose

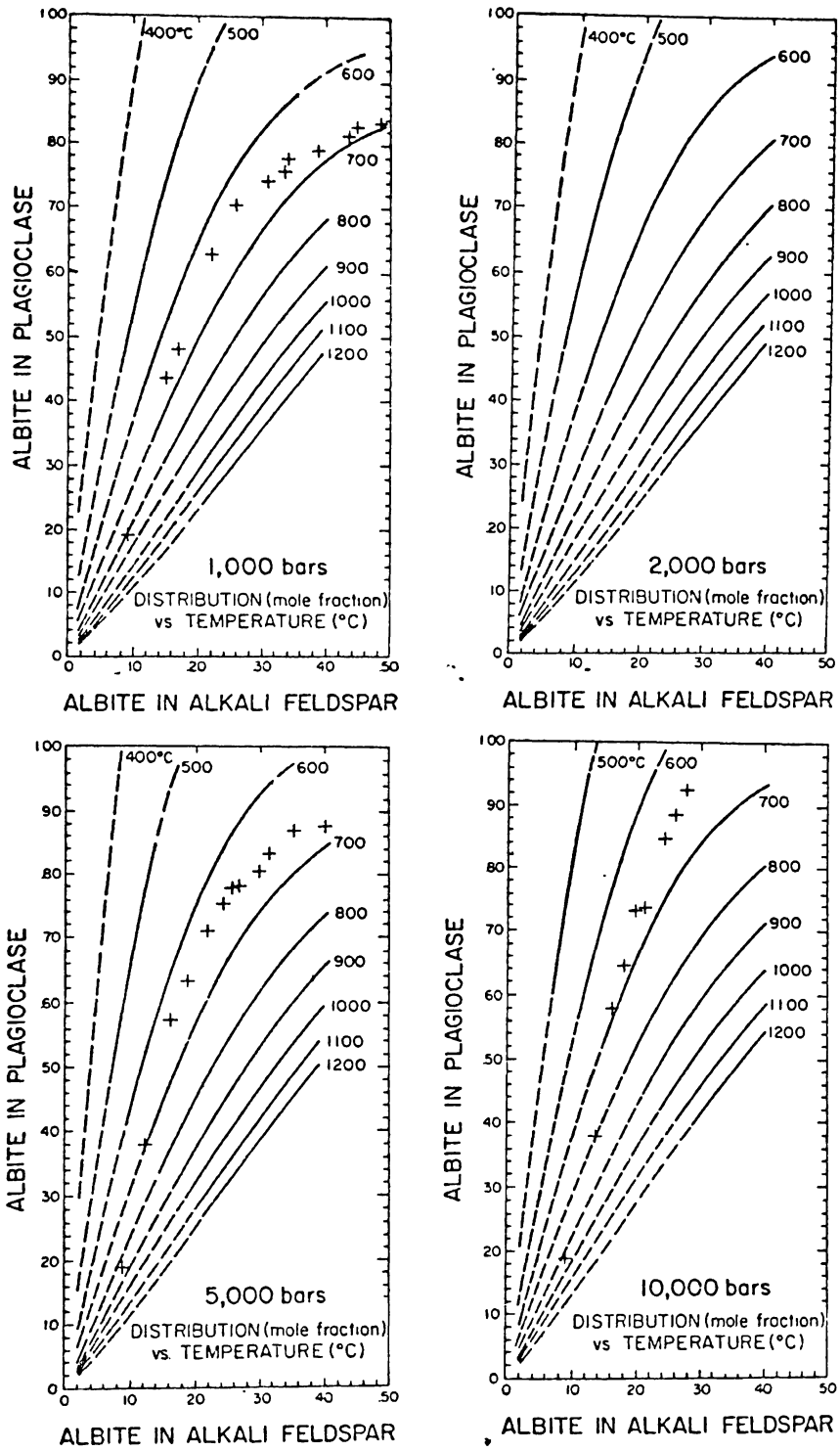


Figure 2: Stormer's (1975) geothermometer.

from. Stormer chose the Margules parameters of Thompson and Waldbaum (1969a, 1969b), which cite independently the contribution to the non-ideality of the alkali feldspar solution made by each of the albite and potash feldspar components. From these parameters Stormer has derived an equation linking the equilibrium temperature at any pressure of a plagioclase and alkali feldspar of any given mole fraction albite:

$$T(^{\circ}K) = \frac{6326.7 - 9963.2X_{af} + 943.3X_{af}^2 + 2690.2X_{af}^3 + (0.0925 - (-1.9872 \ln \frac{X_{af}}{X_{pl}} + 4.6321 - 10.815X_{af} + 0.1458X_{af} + 0.0141X_{af}^2 + 0.0392X_{af}^3)P}{7.7345X_{af}^2 - 1.5512X_{af}^3} \quad (15)$$

From Equation (15), Stormer generated the set of determinative curves shown in Figure (2).

The Stormer (1975) two-feldspar geothermometer has been used with success on epizonal intrusive and extrusive rocks. Three Feldspar-pair temperatures from volcanic rocks from France, Scotland and California (Stormer, 1975), agree with temperatures obtained from Carmichael's (1967) iron-titanium geothermometer. In two of the above comparisons this agreement is within 10°C. Two-feldspar and

iron-titanium geothermometry of epizonal granite intrusives from New Hampshire (Whitney and Stormer, 1976) shows an excellent geothermometric agreement between the quenched rims of the feldspars and the iron-titanium oxides. In addition, internal compositional zones in the plagioclase, in conjunction with the unzoned alkali feldspar yield a series of higher temperatures which are inferred to represent the cooling history of the rocks. The iron-titanium oxides in the rocks evidently re-equilibrated to the falling temperatures until the fluid phase disappeared.

However when two-feldspar geothermometry is attempted on rocks with a longer cooling history, some potential problems loom. Whitney and Stormer (1977a) applied Stormer's (1975) geothermometer with some success to mesozonal granites from Georgia. However they noted that alkali feldspar had locally lost some of its original dissolved plagioclase, which had recrystallized as unzoned oligoclase.

Similarly, Bohlen and Essene (1977), in a geothermometric study on granulites in the Adirondack Highlands, found that both the two-feldspar and iron-titanium oxide mineral associations behaved geothermometrically in a

consistent, reproducible manner. However it was discovered that nonperthitic alkali feldspar has lost a large proportion of its original plagioclase component and had re-equilibrated down to temperatures of 300 to 500°C. Geologically reasonable temperature estimates were achieved only after averaging, for each sample, 100 - 200 point analyses of the perthitic alkali feldspar.

Stormer's geothermometer, like any other, requires a state of chemical equilibrium within its indicator association. Obviously, under any conditions in which plagioclase and alkali feldspar fail to come to equilibrium with respect to albite, or fail to retain that equilibrium, the effectiveness of Stormer's geothermometer will be severely curtailed. The recent work cited above serves as a reminder that equilibrium, if achieved, can later be disrupted.

In adopting the data of Thompson and Waldbaum (1969a, b) Stormer has made three further simplifying assumptions:

- (1) Firstly, Stormer assumes that the parameters he has used are the best available approximation to natural systems. Other formulations for the relevant data give results differing by as much as 100° at some pressures and compositions (for a more complete discussion, and a defence of Thompson and

Waldbaum's data, see Stormer, 1975, pp. 669 - 670). Parsons (1978, p. 204) feels that a better fit to the alkali feldspar-plagioclase solvus is possible than Thompson and Waldbaum have achieved.

A second assumption is necessary if the data of Thompson and Waldbaum are to be used for natural alkali feldspars, as the data are for the Ca-free binary system:  $\text{KAlSi}_3\text{O}_8 - \text{NaAlSi}_3\text{O}_8$ . To deal with the calcium in natural alkali feldspar, Stormer assumes it is ideally dissolved, owing to its dilution. Saxena and Ribbe (1972) found this assumption to be workable; solution properties calculated from experimental data on natural feldspars (Seck, 1971, Orville, 1972) were found to agree closely with those of Thompson and Waldbaum (1969a). The effect, then, of calcium dissolved in alkali feldspar on the mole fraction of albite present is likely to be small, but is at present indeterminate. A similar situation exists with barium and to a lesser extent with the rare earth elements.

Stormer's third assumption in using the data of Thompson and Waldbaum is the least tenable. The Margules parameters used are applicable to sanidine. The assumption that they should be applicable to orthoclase and microcline,

to the infinite number of transitional states between the two minerals, and to perthitic alkali feldspars must be considered with caution.

To correct this weakness, Whitney and Stormer (1977) have recalibrated Stormer's (1975) geothermometer to the thermodynamic properties of microcline. The changes result in an equation similar to Equation (15):

$$T(^{\circ}\text{K}) = \frac{7973.1 - 16910.6X_{af} + 9901.9X_{ab}^2 + (0.11 - 0.22X_{af} + 0.11X_{af}^2)P}{-1.98872 \ln \frac{X_{af}}{X_{pl}} + 6.48 - 21.58X_{af} + 23.72X_{af}^2 - 8.62X_{af}^3} \quad (16)$$

Since Whitney and Stormer's work was published while the present manuscript was in an advanced state of preparation, the majority of geothermometric calculations in this study were performed using Stormer (1975). The results of the two geothermometer with respect to the rocks in this study will be compared in a later section. It suffices here to state that the results of the more recent calibration do little violence to the conclusions herein.

## FIELD AREAS AND REGIONAL GEOLOGY

### Blue Sea Lake Area

The project originally was to proceed in several distinct stages, and was to be launched from a study of a several-square-mile area of medium- or high-grade metamorphic terrain wherein the effects of pressure could cautiously be assumed roughly constant. Subsequent stages of research would proceed in a direction determined by the apparent success or failure of Stomer's geothermometer in the trial field area.

For this field test of the geothermometer, thirteen samples were chosen from a fifteen square-mile area near Blue Sea Lake, Quebec, six miles north of Gracefield (Fig. 3). The samples had been collected in 1969 by Dr. James Bourne in the course of mapping of the Cayamant Lake Area, which was later published as Quebec Department of Natural Resources: Preliminary Report No. 598. The following short description of regional geology is extracted from this report.

The test area lies in the Grenville structural province of the Canadian Shield, and displays considerable evidence of a complicated metamorphic history.

Deformed older rocks show structural discontinuities with younger rocks which themselves show evidence of at least two phases of deformation (deformed foliations, deformed mafic dykes). The older rocks are fine-grained (0.25 mm) gneisses with 15 percent biotite, 55 percent plagioclase, 20 percent potash feldspar, 10 percent quartz and occasional garnet. They are structurally complex, show diffuse lithological contacts and are of uncertain origin, but are tentatively correlated (Bourne, 1970) to Wynne-Edwards' (1969) Grey Gneiss Complex. Most of the exposure in the test area is of the structurally overlying group of marbles, garnet-sillimanite-biotite-feldspar gneisses, and predominantly, garnet-biotite-feldspar gneisses which has been ascribed to the Grenville Group (Bourne, 1970), and has a sedimentary origin.

Of the thirteen samples chosen from the test area, twelve are from Bourne's (1970) garnet-biotite-feldspar gneiss of the Grenville Group. They are typically light pink and medium-grained (1 mm), with augen of potash feldspar as large as 5 mm. Occasional elliptical pods of coarser-grained quartz, potash feldspar and minor plagioclase are approximately 4 cm in diameter.

Foliation is present in all specimens due to mineral alignment and layering, most noticeably of biotite. It also is usually present as preferred orientation of biotite grains and drawing out of quartz grains, and occasionally, as cataclastic attenuation of quartz-feldspar-rich pods. Modes for these samples are: biotite-- 40 percent - 10 percent, plagioclase-- 55 percent - 40 percent, potash feldspar-- 40 percent - 10 percent, quartz-- 15 percent - 10 percent, garnet-- 3 percent - 0 percent. The one sample from the Grey Gneiss Complex is a light grey, unfoliated, strongly lineated gneiss consisting of 55 percent quartz, 35 percent plagioclase, 5 percent potash feldspar and 5 percent biotite.

The prograde mineral assemblage in aluminous Grenville Group gneisses is sillimanite (sometimes coexisting with kyanite)-cordierite-garnet-biotite-plagioclase-alkali feldspar-quartz. The assemblage is stable under high pressure under amphibolite conditions.

Figure 3: Location Map Of Blue Sea Lake Area

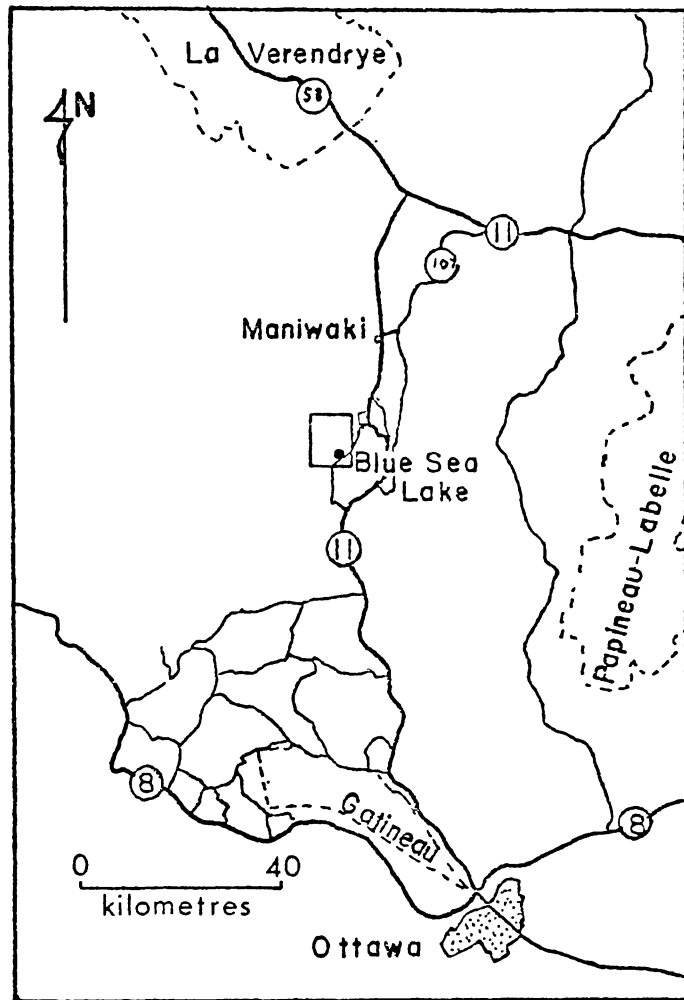


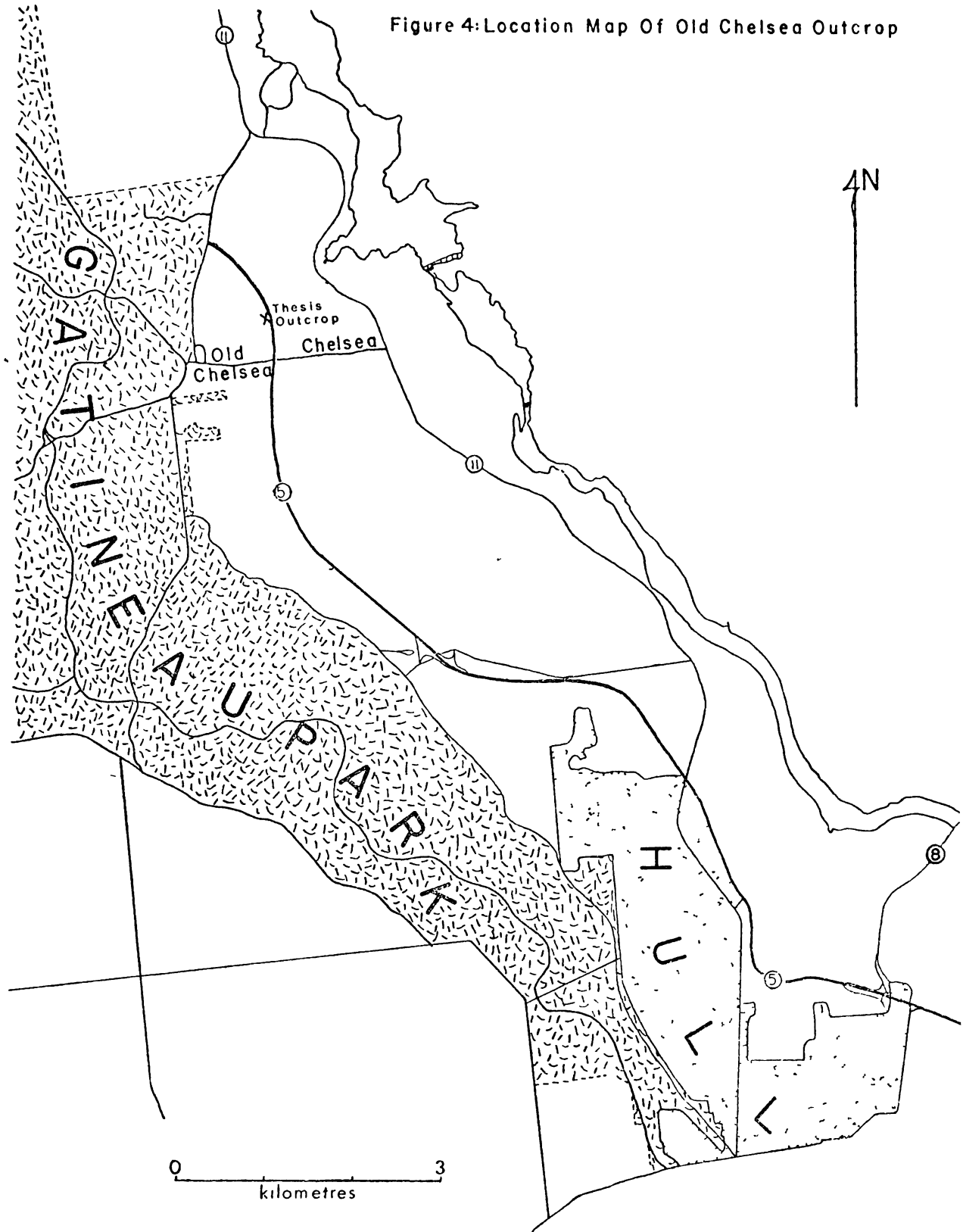
Figure 3: Location of Blue Sea Lake study area. Rectangular box encloses all sample locations (Figure 5). Federal and Quebec Provincial Parks are demarcated by dashed lines.

### Old Chelsea Outcrop

The results of the study in the Blue Sea Lake area necessitated a second phase of research on a single outcrop. This outcrop was chosen from a road cut along the new Number 5 Expressway (Fig. 4) seven miles northwest of the intersection of highways 5 and 8. Extensive mapping of the Parc Gatineau area surrounding the study outcrop by Dr. D. Hogarth was published as Geological Survey of Canada Geological Report 70-a, 1970, from which the following description is abstracted.

The rock of the study outcrop is Precambrian in age and bears a weak foliation imposed by the Grenville Orogeny. The outcrop is part of a homogeneous concordant unit called the Old Chelsea Mass (Hogarth, 1970, map unit 8). It is at least 2,400 metres long, 90 to 275 metres wide and trends sinuously north-south. It is primarily quartz-monzonitic, grading through granodiorite to quartz-diorite (Hogarth, 1970, map units 8a, 8b, 8c, respectively) in the centre of the wider parts of the unit. The mass is believed to have an igneous origin (Hogarth, 1970). The gneissic monzonite of the

Figure 4: Location Map Of Old Chelsea Outcrop



outcrop is intruded by aplitic granite, then by tourmaline pegmatite and finally by diabase. Scarce hornblende and biotite grains in the aplite are oriented to form a foliation.

The mineral assemblage of the Old Chelsea mass, biotite-hornblende-andesine-alkali feldspar, is stable over a very wide range of metamorphic conditions from middle amphibolite grade to granulite. However, orthopyroxene-clinopyroxene-plagioclase-biotite occurs in a mafic rock 300 metres north of the outcrop (Dr. D. Hogarth, pers. comm.). This implies that the maximum metamorphic grade of the study outcrop is at least upper amphibolite facies.

Sixteen samples were taken from the outcrop, with their relative positions accurately noted (Fig. 6, p. 45). Of these, nine were chosen from a portion of the outcrop where the mineralogy and texture appeared in hand specimen to be especially homogenous. Spatially, they form three sets at the apices of a roughly equilateral triangle with a five meter edge. Three samples at the top of the triangle were sectioned from a single large hand specimen, and lie about 10 cm from each other.

These were labelled TT-1, -2 and -3. At the bottom-left corner of the triangle are four samples (LL-1, -2, -3 and -4) taken approximately 50 cm apart. At the bottom-right corner of the triangle lie LR-1 and LR-2, also separated by 50 cm.

The supposedly homogeneous gneiss (considerable modal variability was later discovered, as described in Table 7, p. 79) has a very fresh appearance. It is medium blue-grey with tiny "hairline" streamers of pink alteration and is pyrite-bearing. Intermittent epidote-rich bands 4 cm to 1 metre wide are evidence of greenschist-facies alteration. The gneiss is even-grained without systematic variation in composition, and the fresh surface is not obviously foliated. The weathered surface is typically pink. More precise petrographic data are given below (pp. 78-95). The average modal mineralogy of the gneiss (Fig. 9, p. 85) lies in Streckeisen's (1967) granodiorite field, and the gneiss is hereinafter referred to as the typical granodiorite.

The remaining seven samples were chosen as petrologic variants of the typical granodiorite, and

are numbered V-1 through V-7. There follows a short account of the nature of these variants, with more precise petrography given in a following chapter.

V-1: Even-grained gneiss (V-1 Station 1) similar to the typical granodiorite, but grading into a pegmatitic quartz-feldspar rock (V-1 Station 2) which is rich in very coarse grained (up to 2 cm) potash feldspar. The pegmatite exists as an apparently isolated lens, and contacts with the surrounding gneiss exhibit selvages depleted in alkali feldspar. It has presumably formed by in situ metamorphic differentiation.

V-2: An unfoliated light pink quartz-feldspar pegmatite containing tourmaline, which is not present in the granodiorite. Contacts with the granodiorite are abrupt and the adjacent host rock is not depleted in feldspar. V-2 is not consanguineous with the granodiorite and may or may not have been deformed.

V-3: Epidote-rich gneiss sampled from a strongly-jointed zone approximately two metres wide. It weathers to an intense brick red colour and is a typical granodiorite which was heavily affected by secondary alteration.

V-4: A pink even-grained rock not consanguineous with the typical granodiorite, and occurring near V-3 in the strongly-jointed zone. The rock proved to be devoid of alkali feldspar and was not thin-sectioned.

V-5: A grey-weathering variant of the typical granodiorite entirely devoid of alteration streamers. Mafic minerals are clustered into aggregates roughly 2 cm long. V-5 is a typical granodiorite which appears in hand specimen to have been less subjected to secondary alteration.

V-6: Very similar to the typical granodiorite, but with a slightly pinker overall hue to the feldspars. It was sampled 1.2 metres from the margin of the rock body from which V-7 was taken. V-6 Station 1 is situated on that end of the thin section closest to V-7.

V-7: An alaskitic aplite apparently two metres in diameter showing sharp contacts with the host granodiorite and nonconsanguineous with it.

Hereinafter, samples V-1, -3, -5 and -6, which are petrologic variants of the typical granodiorite, will as a group be referred to as "gneiss variants".

The gneiss variants in conjunction with the typical granodiorite shall comprise the "host gneiss". V-2, V-4 and V-7 will be referred to as nonconsanguineous rocks.

## ELECTRON MICROPROBE ANALYSIS

### Equipment and Technique

Microprobe work was done at Queen's University and was undertaken in two sessions, 17-19 May, and 14-16 June, 1976. The Queen's University microprobe is an Applied Research Laboratories Analyst's microprobe X-ray analyser (ARL/AMX). The apparatus has been tied in to a mini-computer which calculates the necessary Bence-Albee corrections for the raw spectrum counts of each analysis. A corrected analysis is then printed shortly after the raw spectra have been counted.

The energy dispersive mode was used for all analyses. The procedure used to monitor variation in beam current involved counting a spectrum for a quartz standard exactly as is done for an unknown sample. The mini-computer is programmed to compare this spectrum with a standard quartz spectrum stored in memory, and the difference between the two spectra is printed out as a "drift factor". This drift factor is used for all unknown analyses prior to the next quartz standard analysis. An

independent record of the relative beam current intensity is kept by a chart recorder. This is not accurate, but gives the operator a rough idea of the relative stability of the instrument.

Thin sections were well polished to minimize scatter, and were uniformly carbon coated. All sections were rigorously checked for conductivity before analysis; those showing faltering sample current were recoated. The number of unknown analyses done between quartz standard analyses varied from one to four, depending on the stability of the microprobe. Extensive analysis of the Queen's University alkali feldspar standard OR-1 was undertaken with analyses completed at the beginning of each day of probing.

All analyses of unknowns in this study were performed with a beam width of 5 microns. Some standard analyses were performed with a 50 micron beam but a Fischer F-ratio test shows these wide-beam analyses to be not significantly less variable than the narrow-beam analyses.

All analyses were run with a beam current of 35 nanoamps and an accelerating potential difference of 15

Kilovolts. The beam was stationary throughout all analyses.

On the Queen's University microprobe, using the energy dispersive mode and with the 120 second counting period employed for all analyses, detectabilities are at the 0.2 weight percent level for most elements (pers. comm., Dr. Peter Roeder, Queen's University). For the lighter elements, magnesium and sodium, this increases to 0.4 and 0.5 weight percent, respectively.

#### Standard Analyses

In the course of the microprobe analysis, 30 analyses were made of Queen's University's alkali feldspar standard OR-1. This is a sample of adularia from Val Crystallina, Grisons, Switzerland, analysed by Goldich et. al. (1967). For each major oxide except that of barium the analysis of Goldich et. al. (1967) is compared to the average of the microprobe analyses. From Table 1, it can be seen that the microprobe analyses are in excellent agreement with Goldich et. al. with respect to every oxide except that of sodium. The microprobe analyses on the average indicate 0.17 weight percent less  $\text{Na}_2\text{O}$  than does the published analysis, and a Student's "t" test reveals

this disparity\* to be very highly significant. From this it is inferred that all analyses of unknowns will underestimate sodium by 0.17 weight percent  $\text{Na}_2\text{O}$ , or 1.4 mole percent albite.

Also evident from Table 1 is the higher variance (in relation to the amount present) of the sodium analyses. If the variance for sodium in Table 1 is representative of all analyses, then 95 percent of the analyses of unknowns lie within 0.25 weight percent sodium or 2.1 mole percent albite of the true amount present.

This is not a poor performance for such a difficult element, especially in light of the fact that sodium is being dealt with in concentrations barely twice that of its detectability limit.

---

\* This tendency is present only at low concentrations as is revealed by Table 4, p. 49.

Table 1: Reliability Of Standard Probe Analyses.

OXIDE	COMP. OF OR-1 Goldich, et. al. (1967) (WT. %)	AVERAGE OF MICROPROBE ANALYSES (WT. %)	VARIANCE OF MICROPROBE ANALYSES (WT. %)
SiO <sub>2</sub>	64.39	64.14	0.51
Al <sub>2</sub> O <sub>3</sub>	18.58	18.03	0.28
K <sub>2</sub> O	14.92	15.08	0.21
Na <sub>2</sub> O	1.14	0.97	0.13
BaO	0.78	----	----
Others <sup>#</sup>	<u>0.18</u>	----	----
Total	99.99*	98.38	0.84

# 0.03% FeO, 0.035% SrO, 0.03% Rb<sub>2</sub>O, 0.08% H<sub>2</sub>O.

\* Only this total is actually the sum of the values above it.

## Analyses from Study Areas: Recalculation and Tabulation

The results of the microprobed feldspar analyses from both study areas are presented in Table 2. For both feldspars the analyses have been adjusted so that sodium, calcium, and potassium total 100 atomic percent. This assumes that any barium and rare earth elements present in the alkali feldspar are ideally dissolved and act as inert dilutants. For simplicity, Table 2 presents the analyses in a much-abbreviated form. Complete analyses are available from the author upon request.

Since Stormer's (1975) geothermometer is based on a binary solvus, potassium in plagioclase, and calcium in alkali feldspar must also be treated as ideally dissolved inert dilutants. Thus the analyses must be further adjusted so that sodium and calcium in plagioclase, and sodium and potassium in alkali feldspar, total 100 atomic percent. This second adjustment process gives rise to the "corrected" sodium columns of Table 2. The figures tabulated in these columns are the averages for each sample of all acceptable analyses for that sample.

Table 2 : Electron Microprobe Results: Normal Plagioclase and K-feldspar

SAMPLE NO.	ANALYSIS NO.	PLAGIOCLASE ANALYSES*			ANALYSIS NO.	K-FELDSPAR ANALYSES*			EQUILIBRIUM TEMPERATURE (Stormer, 1975) °C
		Na (MOLE %)	K (MOLE %)	AVERAGE** "CORRECTED" Na (MOLE %)		Na (MOLE %)	Ca (MOLE %)	AVERAGE*** "CORRECTED" Na (MOLE %)	
BSL #1	PC-1	69.9	0.9	71.4	KF-1	14.3	0.0	11.8	539
	-2	70.7	1.1		-2	11.0	0.0		
	-3	72.3	0.8		-3	14.0	0.0		
	-4	69.8	0.4		-4	10.8	0.0		
	-5	70.0	1.3		-5	9.1	0.0		
	-6	71.7	1.1		-6	11.8	0.0		
BSL #2	PC-7	75.5	1.0	75.7	KF-7	5.2	0.0	8.4	402
	-8	75.4	0.7		-8	5.4	0.0		
	-9	75.7	1.4		-9	11.9	0.0		
					-10	36.2	0.0		
					-11	35.8	0.0		
					-12	8.0	0.0		
BSL #3	PC-10	74.3	0.6	74.8	KF-13	8.7	0.0	8.9	480
	-11	74.4	1.1		-14	9.2	0.0		
	-12	73.9	1.0		-15	9.0	0.0		
					-16	8.7	0.0		
BSL #4	PC-13	76.5	1.6	77.7	KF-17	6.8	0.0	7.6	450
	-14	77.2	0.6		-18	7.0	0.0		
	-15	77.1	0.9		-19	7.7	0.0		
	-16	78.2	0.5		-20	9.0	0.0		
	-17	75.4	1.7						
BSL #5	PC-18	75.0	1.7	76.2	KF-21	13.0	0.3	13.2	540
	-19	74.5	1.7		-22	12.1	0.0		
	-20	75.9	0.7		-23	14.6	0.0		
					-24	13.1	0.0		

Table 2-1

CU

(33)

Table 2 (cont'd): Electron Microprobe Results: Normal Plagioclase and K-feldspar

SAMPLE NO.	ANALYSIS NO.	PLAGIOCLASE ANALYSES*			ANALYSIS NO.	K-FELDSPAR ANALYSES*			EQUILIBRIUM TEMPERATURE (Stormer, 1975) °C
		Na (MOLE %)	K (MOLE %)	AVERAGE** "CORRECTED" Na (MOLE %)		Na (MOLE %)	Ca (MOLE %)	AVERAGE** "CORRECTED" Na (MOLE %)	
BSL #6	PC-21	71.5	1.5	71.9	KF-25	7.2	0.0	8.8	486
	-22	70.6	0.7		-26	8.9	0.0		
					-27	8.8	0.0		
					-28	10.1	0.1		
BSL #7	PC-23	77.2	0.6	77.6	KF-29	10.2	0.0	10.4	496
	-24	77.0	0.7		-30	10.7	0.0		
					-31	10.2	0.0		
BSL #8	PC-25	70.1	1.3	71.3	KF-32	8.6	0.0	8.7	484
	-26	70.4	1.1		-33	8.7	0.0		
	-27	70.4	1.9						
BSL #9	PC-28	75.3	1.1	75.3	KF-34	15.9	0.0	15.1	567
	-29	74.2	0.8		-35	19.7	0.0		
	-30	74.2	1.1		-36	11.1	0.0		
					-37	13.8	0.0		
BSL #10	PC-31	87.2	0.8	88.8	KF-38	12.5	0.0	9.0	442
	-32	88.2	1.6		-39	6.1	0.0		
	-33	89.0	0.0		-40	8.2	0.0		
					-41	10.7	0.0		
					-42	7.0	0.0		
					-43	8.5	0.0		
					-44	7.2	0.0		
BSL #11	PC-34	72.8	1.1	73.2	KF-45	14.9	0.0	14.0	554
	-35	72.3	0.7		-46	12.7	0.0		
					-47	13.8	0.0		
					-48	15.6	0.0		
					-49	13.2	0.0		

Table 2-2

(#C)

Table 2 (cont'd): Electron Microprobe Results: Normal Plagioclase and K-feldspar

SAMPLE NO.	ANALYSIS NO.	PLAGIOCLASE ANALYSES*			ANALYSIS NO.	K-FELDSPAR ANALYSES*			EQUILIBRIUM TEMPERATURE (Stormer, 1975) °C
		Na (MOLE %)	K (MOLE %)	AVERAGE** "CORRECTED" Na (MOLE %)		Na (MOLE %)	Ca (MOLE %)	AVERAGE*** "CORRECTED" Na (MOLE %)	
BSL #12	PC-36	67.7	0.8	68.2	KF-50	11.2	0.0	9.8	511
	-37	66.6	2.3		-51	13.3	0.3		
					-52	4.9	0.3		
					-53	9.3	0.0		
					-54	10.2	0.7		
BSL #13	PC-38	75.8	0.8	76.3	KF-55	7.3	0.1	8.2	459
	-39	75.9	0.3		-56	12.1	0.3		
					-57	5.7	0.0		
					-58	9.7	0.0		
					-59	7.3	0.7		
					-60	5.8	0.0		
TT-1	PC-40	66.9	1.0	69.1	KF-61	10.3	0.0	8.1	480
	-41	67.1	1.4		-62	7.0	0.0		
					-63	5.6	0.0		
					-64	9.4	0.5		
TT-2	PC-42	66.6	0.5	66.3	KF-65	7.4	0.0	10.4	523
	-43	64.6	1.5		-66	12.4	0.3		
					-67	15.7	0.1		
					-68	8.4	0.0		
					-69	6.4	0.0		
TT-3	PC-44	66.2	0.8	65.9	KF-70	10.2	0.0	9.9	520
	PC-45	64.2	1.3		-71	12.1	0.0		
					-72	9.8	0.0		
					-73	7.6	0.0		
					-74	11.7	0.0		
					-75	8.1	0.0		

Table 2-3

(35)

Table 2 (cont'd) : Electron Microprobe Results: Normal Plagioclase and K-feldspar

SAMPLE NO.	ANALYSIS NO.	PLAGIOCLASE ANALYSES*			ANALYSIS NO.	K-FELDSPAR ANALYSES*			EQUILIBRIUM TEMPERATURE (Stormer, 1975) °C
		Na (MOLE %)	K (MOLE %)	AVERAGE** "CORRECTED" Na (MOLE %)		Na (MOLE %)	Ca (MOLE %)	AVERAGE*** "CORRECTED" Na (MOLE %)	
LL-1					NOT ANALYSED				
LL-2	PC-46	64.4	1.2		KF-76	10.7	0.5		
	-47	64.0	1.2		-77	9.2	0.0		
	-48	63.2	4.4	65.2	-78	13.8	0.0		
	-49	64.7	1.2		-79	6.5	0.2	10.6	
					-80	9.8	0.0	533	
					-81	13.4	0.3		
LL-3	PC-50	64.0	1.4		KF-82	11.1	0.0		
	-51	63.3	0.8	64.3	-83	8.6	0.0		
					-84	8.7	0.0	10.1	
					-85	12.1	0.0	537	
LL-4	PC-52	65.0	1.2		KF-86	10.5	0.0		
	-53	66.7	0.8	66.5	-87	9.2	0.2	9.9	
					-88	10.1	0.0	518	
LR-1	PC-54	65.0	0.1		KF-89	6.0	0.0		
	-55	64.7	0.9	65.3	-90	8.2	0.1		
					-91	8.8	0.0	8.2	
					-92	9.8	0.1	494	
LR-2	PC-56	64.2	1.0		KF-93	6.3	0.3		
	-57	65.8	0.7	65.5	-94	8.1	0.1		
					-95	4.3	0.0		
					-96	8.0	0.0	6.7	
					-97	7.8	0.0	472	
					-98	6.8	0.0		

Table 2-4

(36)

Table 2 (cont'd): Electron Microprobe Results: Normal Plagioclase and K-feldspar

SAMPLE NO.	ANALYSIS NO.	PLAGIOCLASE ANALYSES*			ANALYSIS NO.	K-FELDSPAR ANALYSES*			EQUILIBRIUM TEMPERATURE (Stormer, 1975) °C
		Na (MOLE %)	K (MOLE %)	AVERAGE** "CORRECTED" Na (MOLE %)		Na (MOLE %)	Ca (MOLE %)	AVERAGE*** "CORRECTED" Na (MOLE %)	
V-1 Stn #1	PC-58	65.9	0.9	66.4	KF-99	8.4	0.0	8.6	495
	-59	65.6	1.0		-100	9.1	0.3		
					-101	8.4	0.4		
V-1 Stn #2	PC-60	68.0	0.8	68.3	-102	6.7	0.1	8.2	480
	-61	67.2	1.4		-103	8.4	0.0		
					-104	11.2	1.6		
					-105	6.3	0.1		
V-2	PC-62	98.0	0.3	97.8	-106	3.1	0.0	3.8	338
	-63	95.5	1.1		-107	1.5	0.0		
	-64	97.3	1.1		-108	17.5	0.2		
	-65	84.4	5.6		-109	5.2	0.1		
					-110	5.4	0.4		
V-3	PC-66	95.4	1.3	98.3	-111	8.1	0.0	8.5	424
	-67	99.5	0.5		-112	8.7	0.0		
	-68	98.2	0.0		-113	8.6	0.0		
V-4				NOT ANALYSED					
V-5	PC-69	64.7	0.6	65.6	-114	9.1	0.0	11.3	547
	-70	65.3	1.2		-115	8.9	0.0		
					-116	10.8	0.0		
					-117	18.7	0.4		
					-118	9.3	0.0		
					-119	8.4	0.0		
					-120	14.0	1.3		

Table 2-5

37

(37)

Table 2 (cont'd): Electron Microprobe Results: Normal Plagioclase and K-feldspar

SAMPLE NO.	ANALYSIS NO.	PLAGIOCLASE ANALYSES*			ANALYSIS NO.	K-FELDSPAR ANALYSES*			EQUILIBRIUM TEMPERATURE (Stormer, 1975) °C
		Na (MOLE %)	K (MOLE %)	AVERAGE** "CORRECTED" Na (MOLE %)		Na (MOLE %)	Ca (MOLE %)	AVERAGE*** "CORRECTED" Na (MOLE %)	
V-6 Stn #1	PC-71	68.4	0.0	67.9	KF-121	7.0	0.0	6.4	458
	-72	65.3	0.2		-122	5.8	0.0		
	-73	71.0	1.0						
	-74	63.7	0.3						
	-75	69.9	0.0						
V-6 Stn #2	-76	62.4	0.9	63.2	KF-123	8.4	0.0	9.1	530
	-77	62.8	1.1		-124	13.6	0.1		
					-125	9.1	0.4		
					-126	7.9	0.0		
					-127	11.2	0.0		
					-128	7.0	0.0		
V-7	-78	98.7	0.3	99.0	KF-130	5.7	0.0	5.5	374
					-131	6.5	0.0		
					-132	4.4	0.0		

Table 2-6

LEGEND

- \* Corrected so the three major elements Na, Ca and K total 100 mole per cent.
- \*\* Corrected so Na and Ca total 100 mole per cent.
- \*\*\* Corrected so Na and K total 100 mole per cent.
- † Analyses enclosed within curly bracket are from exactly the same location.
- †† Average in plain brackets includes the anomalous analyses enclosed in rectangular boxes.

Table 3: Electron Microprobe Results: Exsolved Plagioclase and K-feldspar

SAMPLE NO.	ANALYSIS NO.	PLAGIOCLASE EXSOLVED FROM K-FELDSPAR			ANALYSIS NO.	K-FELDSPAR EXSOLVED FROM PLAGIOCLASE		
		Na (MOLE %)	Ca (MOLE %)	K (MOLE %)		Na (MOLE %)	Ca (MOLE %)	K (MOLE %)
BSL #9	PC-79	25.3	3.1	71.5				
BSL #13	-80	78.4	20.6	1.0				
	-81	72.1	20.7	1.2				
TT-3	-82	35.5	6.1	58.4				
LL-3	-83	66.2	31.8	2.0				
	-84	36.7	9.1	54.2				
	-85	20.1	1.0	78.9				
LR-2	-86	17.0	1.9	81.1				
	-87	65.8	12.6	21.6				
	-88	30.8	3.3	66.0				
V-1	PC-89	65.9	33.4	0.8				
	-90	11.2	1.6	87.2				
V-3					KF-133	6.4	0.7	93.3
					-134	2.8	0.8	96.3
					-135	5.4	0.0	94.6
					-136	4.3	0.0	95.7
					-137	7.1	0.0	92.9
					-138	2.8	0.0	97.2
V-6	PC-91	38.6	6.2	55.2				
	-92	60.3	11.4	18.2				
	-93	69.3	12.5	12.2				
	-94	99.0	0.5	0.5				
V-7	PC-95	79.7	5.8	14.6				
	-96	22.9	2.4	74.7				

W  
6

(-39)

The average "corrected" sodium values for each sample were substituted into a computer program which calculates the solution of Equation 15 over a range of pressures. The solution tabulated assumes a containing pressure of 6400 bars.

#### Microprobe Data: Blue Sea Lake Area

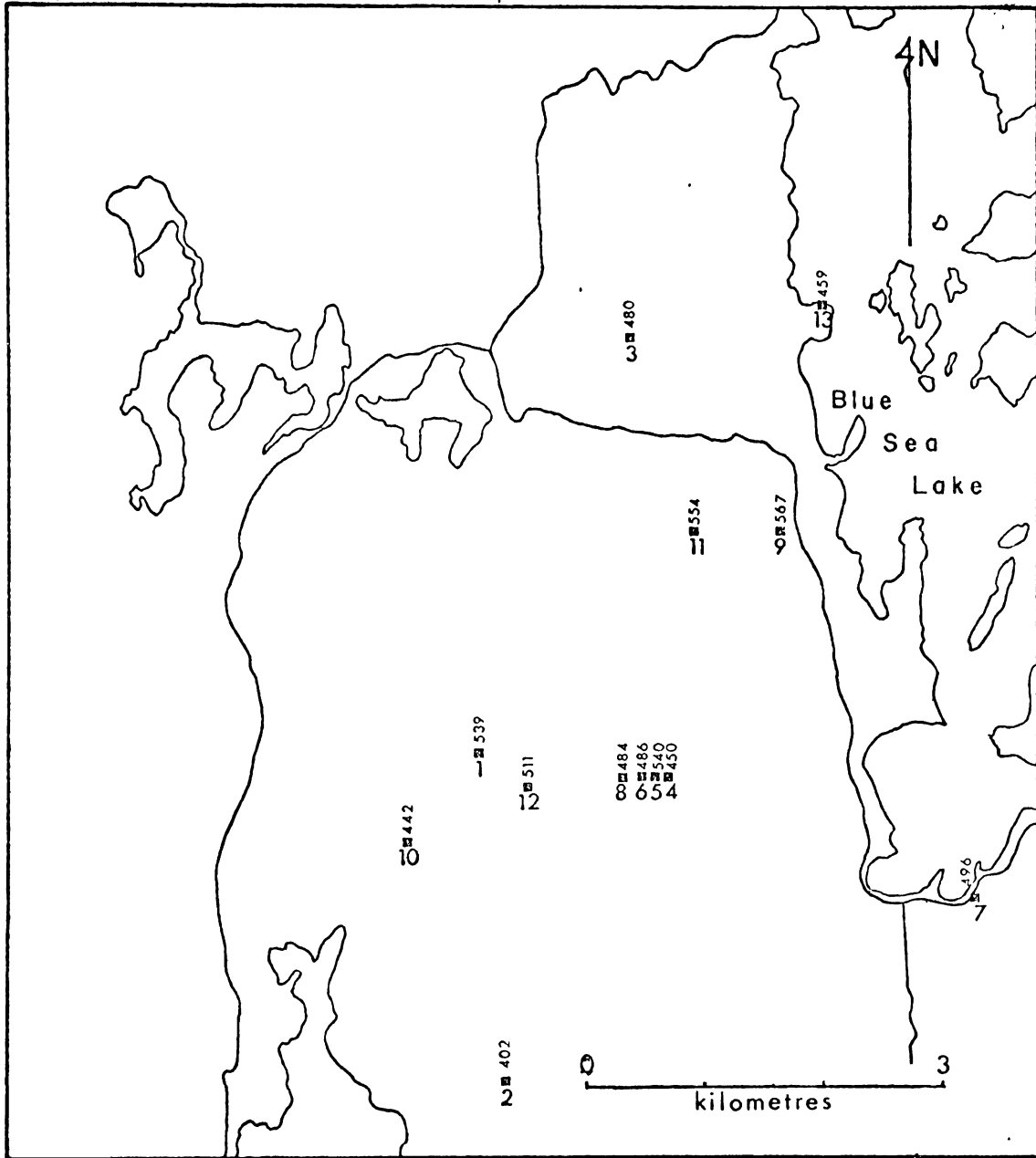
Stormer's estimated metamorphic temperatures for the Blue Sea Lake area samples, arrived at using the simplistic approach outlined above, are shown in Table 2, and their spatial distribution is displayed in the map of Figure 5. As is discussed below, the results show considerable variability, with estimated temperatures ranging from 402 °C to 567 °C. Nor is there any apparent pattern to the spatial distribution of these temperatures. Furthermore the average temperature of 493 °C is about 100-150 degrees too low for the middle-to-upper amphibolite facies conditions, inferred from Bourne, 1970.

#### Microprobe Data: Old Chelsea Outcrop

The results of two-feldspar geothermometry in the Blue Sea Lake area made evident the need for a more detailed study. Accordingly, from June 14 to June 17, 1970

Figure 5: Detailed view of Blue Sea Lake study area (as located in Figure 3). Metamorphic equilibration temperatures according to Stormer (1975) are shown as vertical superscripts.

Figure 5: Blue Sea Lake Sample Locations

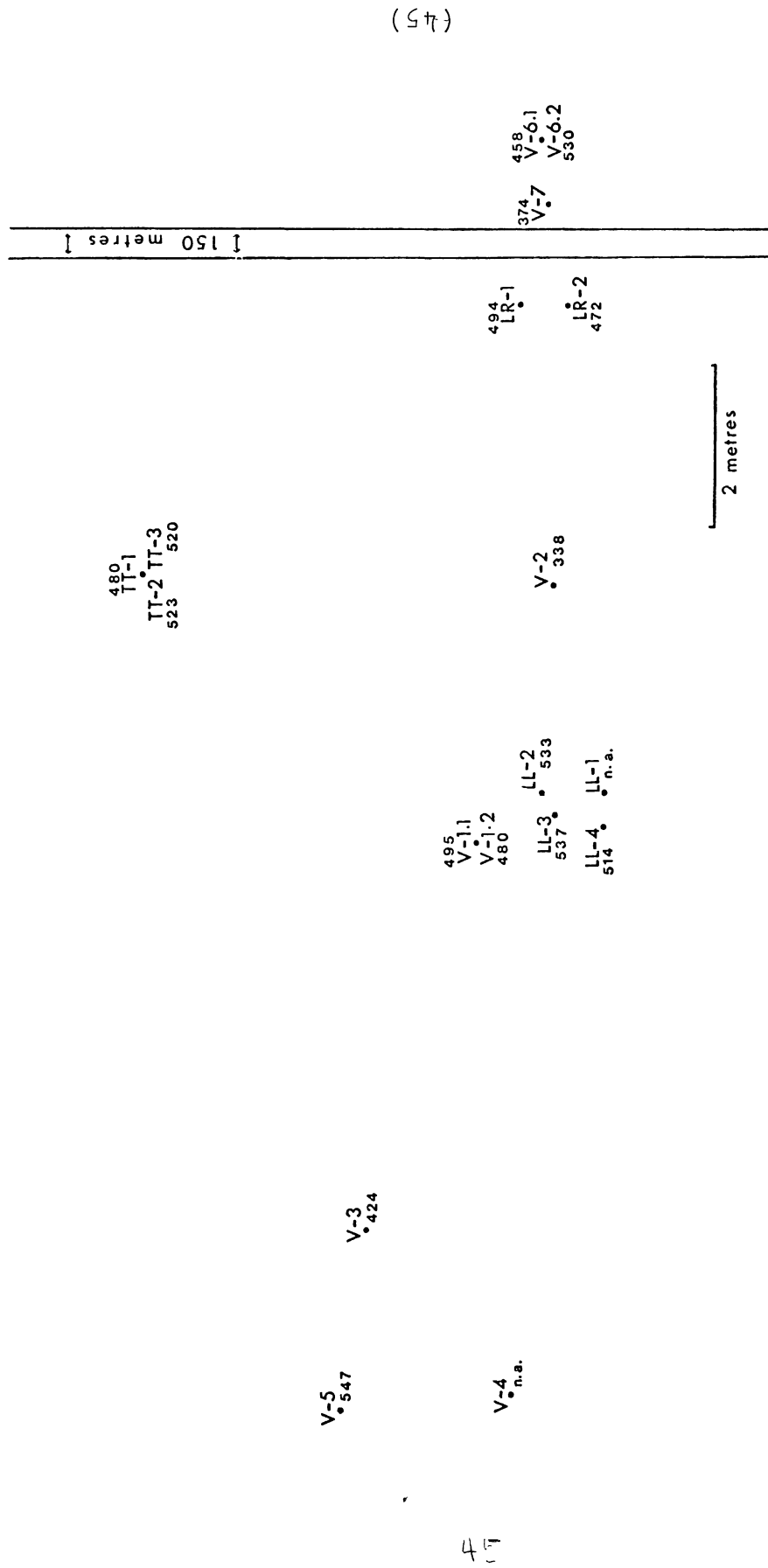


feldspar analyses were made of 14 samples taken from a single large outcrop. These samples were taken with two purposes in mind: 1) to delimit the scale of variation in Stormer's estimated equilibrium temperatures 2) to determine the extent and character of variation of these temperatures with rock type.

The analyses are tabulated (Table 2) in the same format used for the Blue Sea Lake data, and the results of a similar simplistic "data-averaging" application of Stormer's geothermometer are shown in Figure 6. As in the Blue Sea Lake area, considerable variability is present within each sample (Table 2) and this variability is expressed when one attempts to use the mean of each sample's analyses for geothermometric purposes. Moreover the average of these temperatures (excluding the obviously intrusive rocks represented by V-2 and V-7) is, at 503 °C, not appreciably higher than that for the Blue Sea Lake area. This is at least 150 degrees lower than the maximum ambient temperature extant during the metamorphism of the Old Chelsea Outcrop.

Figure 6: Detailed view of Old Chelsea outcrop study area, as located in Figure 4. Metamorphic equilibration temperatures according to Stormer (1975) accompany sample locations. "n.a." accompanies samples not analysed.

Figure 6: Relative Positions Of Old Chelsea Outcrop Samples



### Discussion of Old Chelsea Outcrop Data

From the temperature estimates in Figure 6, two qualitative geothermometric successes can be inferred. Firstly the gneiss variants and non-consanguineous samples with Stomer temperatures ranging between 338 and 547°C, show greater variation than that within the typical granodiorite samples, which vary only within the range of 472° to 537°C. The feldspars evidently reflect at least something of the wider range of petrologic conditions to which they have as a group been exposed. Secondly, if the granodiorite samples at each apex of the triangle are considered as separate groups, there is perhaps less variation within those groups than between them. This implies that superimposed on the above-mentioned small scale variation, is a non-uniformity with a scale of several metres. However it must be said that the evidence for even these humble successes is not compelling.

### Discussion of Microprobe Data

Apparent in the analyses presented in Table 2 is the extreme variability of sodium content in the alkali feldspar, which persists despite the close spacing of the analyses. For most samples only one alkali feldspar grain

was analysed, and analyses KF-7 and KF-9 are only 100 microns apart.

At least some of this variation must be due to real inconstancy of composition in the alkali feldspar. In BSL-10, analyses KF-42, -43, and -44 are from exactly the same location and have a much lower variance than analyses KF-38 to -41 inclusive, which were performed elsewhere in the same mineral grain. Further examples are the two pairs of analyses KF-7 and -8 and KF-10 and -11, performed at two locations within a single alkali feldspar crystal. Note the strong agreement within each pair and the great disparity between the two pairs.

Further, in comparing the analyses of OR-1 to those of the Old Chelsea outcrop samples, one notices a great difference in variance. Variance of the standard analyses is less than 14 percent of the amount present; that of the Old Chelsea outcrop specimens is over 23 percent of the amount present. A Fischer F-ratio test discloses that this difference is very highly significant. Therefore at least some of the variability in the alkali feldspar analyses from the study areas must represent real inhomogeneity in sodium content.

Let us, on an individual sample basis, compare the variability in the alkali feldspar analyses to their uncertainty ( 2.1 percent albite at 95 percent confidence, p.30), as estimated from the standard analyses. Analyses from samples such as BSl no. 3, no. 7, and LL-4 show variation well within this uncertainty interval and these samples may well be homogeneous. Analyses from others, like BSL no. 10 and LL-3, are much less uniform, and some of this variability must reflect actual inconstancy in sodium content.

However it is uncertain whether this inconstancy results from non-uniformity in the amount of sodium dissolved in the host phase of the alkali feldspar, or to the impingement of the microprobe beam upon small lamellae of exsolved plagioclase. Probably both are in part responsible.

Analyses of plagioclase are much less divergent than those of alkali feldspar, and results agree closely with optical anorthite determinations (Table 4).

Geothermometric expression of the uncertainty in the alkali feldspar analyses will vary according to the

Table 4: Na In Plagioclase: Probe vs Optics

SAMPLE NO.	MOLE % Na IN PLAGIOCLASE	
	OPTICAL DETERMINATIONS	ELECTRON MICROPROBE*
BSL-1	72	70.7
BSL-2	76	75.5
BSL-3	76	74.2
BSL-5	76	75.1
BSL-6	70	71.0
BSL-7	76	77.1
BSL-8	72	70.3
BSL-9	77	74.6
BSL-11	66	72.6
BSL-12	66	67.1
BSL-13	77	75.9

\* Average of uncorrected results (Table 2)

compositions of the feldspars and according to the assumed containing pressure. An average feldspar pair from the host gneiss of the Old Chelsea outcrop (calculated by averaging all relevant analyses in Table 2) contains 9.2 and 69 percent albite in the alkali feldspar and plagioclase, respectively. For these feldspars, at an assumed pressure of 6400 bars, a 2.1 mole percent uncertainty in alkali feldspar composition is equivalent to an uncertainty interval of 27° C in equilibration temperature. Thus, as a safe working figure, the data can be stated to be accurate within 30° C at 95 percent confidence, ignoring the small effect of the uncertainty in plagioclase composition.

It has also been inferred (p.30) that the micro-probed alkali feldspar analyses underestimate sodium concentration by an amount equivalent to 1.4 percent albite. A computation very similar to the one immediately above indicates that equilibration temperatures inferred from the analyses are about 25° C too low.

The average of estimated maximum metamorphic temperatures for the Old Chelsea outcrop samples is 503° C

(p.43). If one corrects for the consistent analytical error in alkali feldspar composition this average temperature becomes  $537^{\circ}$  C; still geologically unreasonable. However Stormer's (1975) geothermometer is based on the thermodynamic properties of sanadine, and its applicability to perthitic microcline is limited. If we then employ Whitney and Stormer's (1977) model as represented by Equation 16, p.15), which is based on the properties of microcline, the estimated maximum metamorphic temperature climbs to  $567^{\circ}$  C. This is of course an improvement but is still as much as  $100^{\circ}$  C lower than the maximum metamorphic temperature attained by the host gneiss of the study outcrop.

Let us now turn to sample BSL no. 5, whose relatively uniform analyses average 13.2 percent albite. If this value is corrected for analytical error and substituted into Equation 16, the result obtained is an encouraging  $625^{\circ}$  C. This is still perhaps low, but is a geologically reasonable result.

Thus it seems that with patience and extensive analyses and sampling, geologically reasonable geothermometric results can be obtained from analysis of

polydeformed plagioclase and perthite. However the great effort and expense required to obtain this result certainly argues against the casual application of this geothermometer under these conditions.

So far discussion has centered on the sodium content of the host phase of the alkali feldspar which, in conjunction with the composition of the coexisting plagioclase, should have equilibrated to conditions extant at the maximum grade of metamorphism. It is of interest however to consider the highest temperature which can be obtained by combining the estimated sodium content remaining dissolved in an alkali feldspar sample and the point-counted modes of exsolved plagioclase within that sample. (presented in Table 9, p.122). The temperature estimate thus obtained should provide a clue to the ambient temperature during the crystallization of what is now the host gneiss from its original magma.

Temperature estimates obtained using point-counted exsolved plagioclase estimates combined with microprobe analyses cannot be as accurate as the values presented in Table 2, as they incorporate the error in both analytical methods. It is known for example (p.77), that the exsolved plagioclase estimates may be too large. In

addition the large amounts of calcium in the exsolved andesine lamellae must introduce some error as neither Stormer (1975) nor Whitney and Stormer (1977) rigorously attack the problem of calcium dissolved in alkali feldspar. However the results are nonetheless interesting.

Stormer's (1975) geothermometer estimates the primary igneous temperature of V-5 to be 865~ C, which is perhaps high but is plausible. However Whitney and Stormer (1977) estimate this temperature to be 1097° C, which is much too high for a granodiorite pluton.

Thus geothermometry implies that the alkali feldspar crystallizing from the original magma of the Old Chelsea pluton was disordered, and subsequently became ordered before or during the highest grade of metamorphism of the host gneiss.

## OIL IMMERSION STUDY

### Introduction

The microprobe data from both test areas indicate considerable small-scale variability in the alkali feldspar composition. At this juncture the author felt the need to independently corroborate this variability. However, aside from electron microprobe spectroscopy, very few analytical techniques are extant which do not require homogenization of the sample. Most optical analytical methods (measurement of optic axial angle and of extinction angles to 001 and 010) are inaccurate unless used in conjunction with X-ray diffraction techniques (Stewart, 1976). It was therefore decided to undertake an oil immersion study.

### Method Employed

The standard oil immersion technique for finding the composition of a mineral in a solid solution series involved a comparison between the refractive index (or refringence) of a mounting oil to that of a chosen optical direction in the sample grains of the mineral. By a series of such comparisons, the refringence of the mineral is circumscribed into an ever-narrowing interval. The

inadequacies of this technique are twofold. Firstly, it is prohibitively slow. Secondly, for each sample analysed, the refringence of the mineral grains is accurately known in only a small fraction of the prepared oil mounts. Knowledge of small-scale variation within each sample can be gleaned only with great difficulty.

Since a large number of oil immersion data were needed, an innovation was made on this standard technique. The author's technique involves interpolating between the extremes of refringence of a mineral grain with a known orientation mounted in an index oil of intermediate refringence. Figure 7 diagrammatically explains the procedure. In the example of Figure 7 this orientation is a centered obtuse bisectrix figure with  $\alpha$  and  $\beta$  in the plane of the stage. When a grain of the desired orientation is found (its refringence should vary from greater than to less than that of the oil mount) it is rotated until, in monochromatic light, the Becke line splits or disappears entirely. The angle between this minimum relief orientation and the optic axis of lower refringence is then measured.

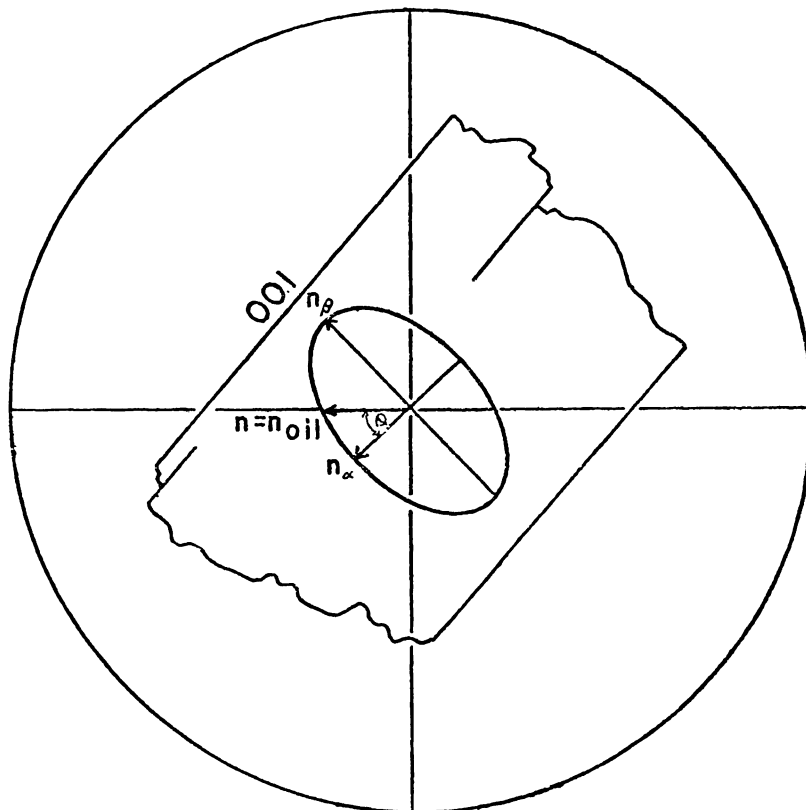


Figure 7: Refringence relationships of a sample grain of microneedle mounted in immersion oil. The grain, yielding a centered obtuse bisectrix figure, is shown in its minimum relief position in the oil.

This method hinges on a solution for the way in which the refringence ( $n$ ) of the oriented grain in question varies upon rotation (the angle  $\theta$  in Fig. 7). Now,  $n$  must vary according to the formula of an ellipse whose unique axes are, in our example, the principal vibration directions  $\alpha$  and  $\beta$  (Fig. 7):

$$n = \sqrt{\frac{\alpha^2 \beta^2}{\sin^2 \theta \alpha^2 + ((1 - \sin^2 \theta) \beta^2)}} \quad (17)$$

where  $\theta$  is the angle of the grain from its point of extinction to  $\alpha$  in the maximum relief orientation.

Now if one knows the  $\alpha$  and  $\beta$  values for both end member compositions of the solid solution series (in this case, potash feldspar and albite), computations similar to that of Equation 17 can be performed to find the refringence of each end member composition at a particular  $\theta$  value:

$$n_{Ab} = \sqrt{\frac{\alpha_{Ab}^2 \beta_{Ab}^2}{\sin^2 \theta \cdot \alpha_{Ab}^2 + ((1 - \sin^2 \theta) \beta_{Ab}^2)}} \quad (18)$$

$$n_{Kf} = \sqrt{\frac{\alpha_{Kf}^2 \beta_{Kf}^2}{\sin^2 \theta \beta_{Kf}^2 + ((1 - \sin^2 \theta) \beta_{Kf}^2)}} \quad (19)$$

where the subscripts Kf and Ab refer to the potash feldspar and albite end members, respectively.

Now, in the minimum relief orientation of the sample grain (Fig. 7) where the refringence ( $n$ ) of the grain equals that of the oil and  $\theta$  is known,  $n_{Kf}$  and  $n_{Ab}$  can be calculated from equations (18) and (19), and substituted into Equation (20) to find the mole fraction ( $X_{Kf}$ ) of potassium in the sample grain:

$$X_{Kf} = \frac{n_{Ab} - n_{Oil}}{n_{Ab} - n_{Kf}} \quad (20)$$

The refringence values for the alkali feldspar solution series were adopted from the data of Tuttle, 1952 (in Deer, Howie and Zussman, 1966, p. 309), for orthoclase-low albite.

A computer program has been written which performs the calculations of equations (18), (19) and (20). The program is usable for any solid-solution series where refringence varies linearly with composition. It is also applicable to known grain orientations oblique to the principal vibration directions, and is available from the

author on request.

The optical system used for the study was a Zeiss Student microscope with light reflected from a sodium vapour source.

Two grain orientations were used for all refringence determinations. From a grain lying on the 010 cleavage, a centered obtuse bisectrix figure (BXO) is obtained, with  $\alpha$  and  $\beta$  lying in the plane of the stage. The other principal cleavage, parallel to 001, yeilds an off-center flash figure. The obliquity of this latter orientation was calibrated on a flat stage microscope from the polished thin sections of Old Chelsea samples V-1 and LL-2 in the following manner. Since an 010 cleavage fragment is known to yield a centered BXO,  $\beta$  must parallel crystallographic b, and since 001 $\wedge$ 010 in classical microcline is 90 $\sim$ 18', in a centered BXO orientation 001 will be effectively perpendicular to the stage, and  $\beta \wedge 001$  can be measured without distortion. From the two samples used, 10 centered BXO's were obtained and the angle was measured between the fast ray and the 001 cleavage trace. The average of these results is 82.3 degrees. In a 001 cleavage fragment the slow ray effectively equals  $\beta$ .

To estimate the refringence of each sample, approximately 100 grains of alkali feldspar, crushed to about 0.05 millimeters in diameter, were placed on a very clean slide and covered with a fragment of thin cover glass. The index oil to be used was calibrated to four decimal places with a refractometer, and inserted under the cover glass of the prepared slide by capillary action. Grains in the mount were then checked for proper orientation, sparseness of perthite, and a clear Becke line. Each suitable grain was then rotated with extreme caution until, when the stage was racked, the Becke line split into two lines of equal intensity which were always equidistant from the grain boundary. If the Becke line was not symmetrical in the minimum relief position of the grain, the grain was rejected. If the Becke line split properly, the angular orientation on the stage vernier of the minimum relief orientation was noted. Also noted was the angle at which, in the area of the split Beck line, the fast ray was parallel to the lower polarizer, and the difference between these two angles was recorded.

#### Discussion of Method

The above-described method has four major shortcomings

which lessen the method's effectiveness when used on alkali feldspar solid solutions. 1) The low birefringence of alkali feldspar and the relatively small difference in refringence between its two end-members lowers the potential accuracy the method would have on other solid solutions. 2) The presence of exsolved plagioclase and the fine "patchwork" twinning combine to lower precision and to drastically reduce the number of acceptable sample grains in each mount. 3) In non-binary solid solutions such as alkali feldspar, the refringence of the analysed sample is affected by non-binary dissolved components and these effects are not determinable by this method. 4) The need for extreme care in the determinations precludes rapidity.

Despite the above disadvantages, this modification of standard oil immersion technique is usable on any non-isotropic mineral with cleavage either lacking or in known orientations. If non-binary dissolved components are a potential problem, some control must be gained from another method such as atomic absorption spectroscopy. Once this is done, however, quantitative results should be possible on any solid solution series whose variation

of optics with composition is known, and this method is sensitive to small-scale inhomogeneity.

#### Calibration of Method

To determine the potential precision and accuracy of the method, the author made twelve determinations of the refringence of quartz, using the technique described above.

Each determination was made in the following way. A mounted grain in a maximum birefringence orientation (i.e. yielding a centered flash figure) was found, so that upon a  $90^\circ$  rotation of the stage the refringence of the grain would vary between 1.54425 ( $\omega$ ) and 1.55336 ( $\epsilon$ ). The stage was then rotated until the grain was judged to be in its minimum relief position in the mounting oil. The angle between the minimum relief position of the test grain and extinction at the minimum refringence position ( $\omega$ ) was recorded. This is the  $\mathcal{O}$  value for the test grain. The grain was then rotated in small increments to either side of its estimated minimum relief position in order to determine for each grain the size of the angular interval within which the Becke line was not visibly asymmetric.

This interval indicates the smallest change in refringence visible to the eye while using this technique, and hence represents the limits of precision of the technique.

The actual accuracy of the technique was quantified in the following manner. The computer program was modified to calculate, from the  $\theta$  value for each determination and the known refringence of quartz, the actual refringence of the quartz grain in its estimated minimum relief orientation. This calculated refringence will ideally equal the refringence of the mounting oil. Therefore a graph of the calculated refringence of the quartz grain versus the refringence of the mounting oil should generate a straight line of unit slope. The quartz calibration data are presented in this format in Figure 8. The shorter of the two sets of error bars for each point represents the above-mentioned limits of precision of the method, expressed in terms of refringence.

Each determination was made in one of four index oils which were calibrated on the refractometer to the following refringences: 1.5458, 1.5460, 1.5490 and 1.5513. Repeated use of the refractometer disclosed a variance of 0.0002 in its refringence measurements. This

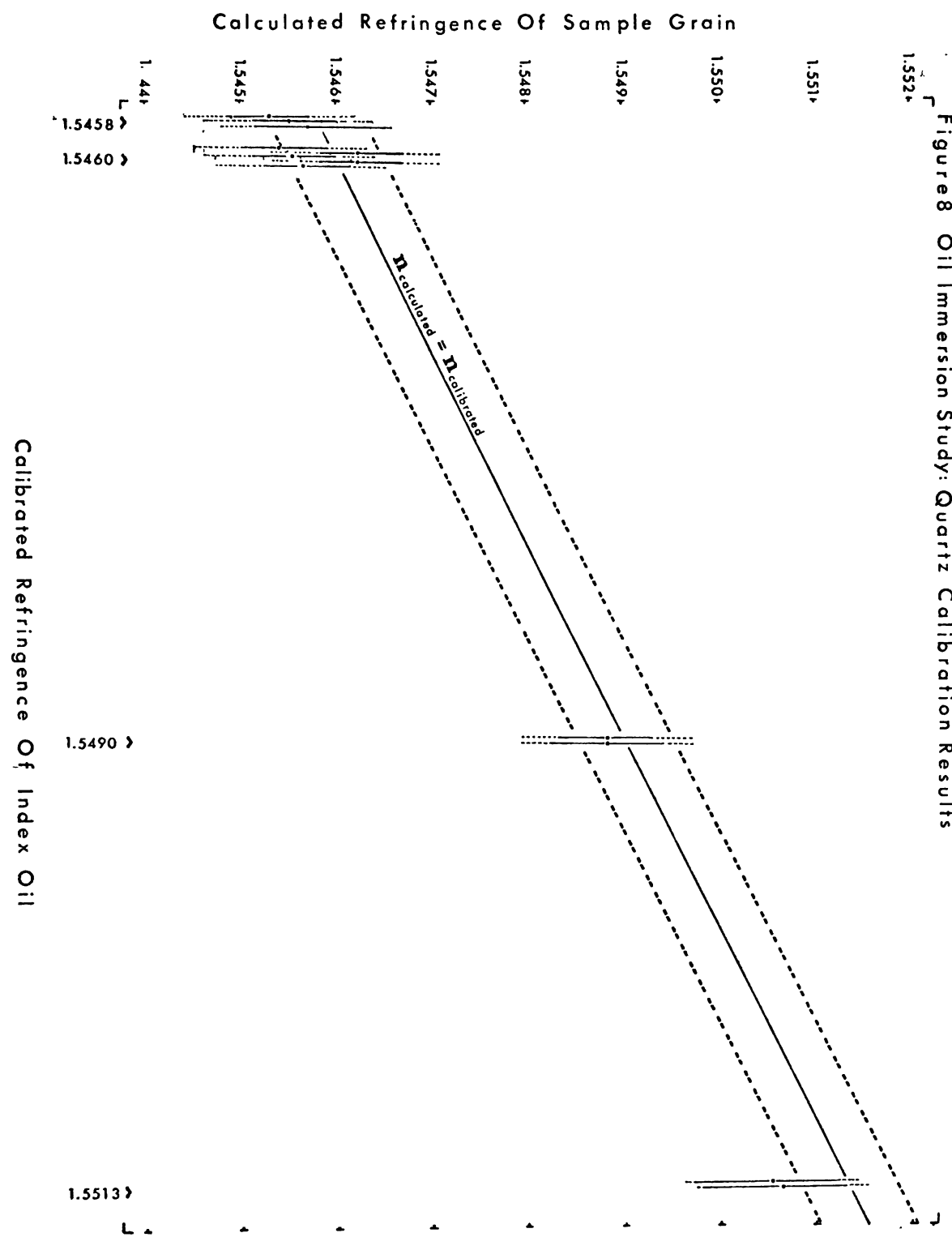
variance was used to delimit a 95 percent confidence interval (shown by the dashed lines in Figure 8) in the calibration of the mounting oils.

From Figure 8 it can be seen that all the data are easily accurate to within the total uncertainty of the technique, but that most of the calculated quartz refringences are low. This is due to the cold room in which the determinations were carried out. With the refractometer and the index oils equilibrated to a temperature of about 20°C, the heat from the sodium lamp caused the refringence of the mounting oils to drift downwards during the determinations. Nor was this effect measurable, since during attempts to measure the refringence of the oil after each determination, the refractometer quickly cooled the oil back down to room temperature. However, from the data it can be seen that the effect of oil drift was fairly small.

From the discrepancy between observed and expected results, the variance of the data is calculated to be 0.00047. Therefore, at 95 percent confidence, the technique is accurate to within  $\pm 0.0009$  (shown in Figure 8 as the longer of the two sets of error bars). It is potentially precise to within  $\pm 0.0004$  in its refringence measurements.

Figure 8: Quartz calibration data achieved by observing the values of oil-mounted quartz grains yielding flash figures. For each sample grain the  $\theta$  value was substituted into Equation 17 (p. 57) to calculate its refringence ( $n$ ) in the minimum relief position in the oil. Solid error bars about data points are the subjectively determined limits of precision of the technique (p. 64). Dotted error bars delimit the statistically determined 95 percent confidence interval in the data. Dashed lines delimit the 95 percent confidence interval in calibration of the oil index.

Figure 8 Oil Immersion Study: Quartz Calibration Results



## Data

Over fifty acceptable determinations were made with the above-described oil immersion technique on five samples from the Old Chelsea outcrop. The data are presented in Table 5, and are seen to be excessively variable. Now, the birefringence of the alkali feldspar solid solution is very low, and the difference in refringence between the two end-members is small. As a result, the experimental error of  $\pm 0.0009$  in refringence measurements made using the above method manifests itself as an uncertainty in mole fraction of 8 mole percent albite. The variation within the data for some samples (i.e. TT-3) exceeds the estimated experimental error, but the precision of the technique must be some amount lower for twinned perthite than for quartz. Thus it is difficult to discern the extent to which the variability is controlled by real variation in composition of the alkali feldspar host. The data for the alkali feldspar of sample V-2 reaffirms the sample's low Na content as discovered by the probe analyses, but the author's technique must nonetheless be considered a failure at its first appointed task. However, it is submitted that better results would be obtained if the technique was used on a solid solution series with a higher birefringence.

Table 5: Results of Oil Immersion Study: K-feldspar of Old Chelsea Outcrop

SAMPLE NO.	ANALYSIS NO.	Na IN K-FELDSPAR (MOLE %)	SAMPLE AVERAGE	EQUILIBRATION TEMP. (Stormer, 1975). °C	SAMPLE NO.	ANALYSIS NO.	Na IN K-FELDSPAR (MOLE %)	SAMPLE AVERAGE (MOLE %)	EQUILIBRATION TEMP. (STORMER, 1975). °C	
TT-1	OI-1	15.5	16.0	605	TT-3	OI-26	15.8	13.5	581	
	-2	17.3				-27	14.1			
	-3	9.3				-28	14.1			
	-4	20.0				-29	11.3			
	-5	17.8				-30	9.7			
	-6	17.2				-31	9.9			
	-7	19.5				LR-2	OI-32			17.4
	-8	18.6					-33			10.6
	-9	11.7					-34			14.7
	-10	14.0					-35			14.9
TT-2	OI-11	13.0	13.1	571	-36	18.7				
	-12	10.1			-37	16.5				
	-13	11.4			-38	13.8				
	-14	10.6			-39	15.2				
	-15	20.2			-40	11.7				
TT-3	OI-16	20.5	14.2	587	V-2	OI-42	14.9	10.6	446	
	-17	24.9				-43	14.9			
	-18	15.1				-44	19.4			
	-19	15.6				-45	1.9			
	-20	16.8				-46	8.7			
	-21	14.5				-47	12.5			
	-22	16.4				-48	7.9			
	-23	6.2				-49	14.9			
	-24	17.9				-50	2.7			
	-25	3.9				-51	7.9			

85

(68)

In addition to their extreme variability, the oil immersion data, averaging 14.3 mole percent albite (not including data for V-2), are about six mole percent higher than the average of the microprobe data (8.4 mole percent, from Table 1) for the same samples. Recall, however, that the quartz calibration data in Figure 8 indicate a non-measurable lowering of the index of the immersion oil during the determinations. The data best fit a line corresponding to a refringence depression of 0.0006. This in turn corresponds to an average albite overestimate of five mole percent. Thus oil drift is in itself an adequate explanation of the disparity between the two modes of analysis.

## ATOMIC ABSORPTION SPECTROSCOPY

### Method of Analysis

Atomic absorption spectroscopy was undertaken primarily to learn the extent to which barium is present in the feldspars of the Old Chelsea outcrop. From five specimens of the Old Chelsea outcrop, eight alkali feldspar concentrates were prepared. The concentrates were prepared simply by prying loose and crushing small crystals of pure alkali feldspar, and were carefully checked for purity under a binocular microscope in an effort to minimize plagioclase contamination. The samples to be analysed were chosen entirely on the availability of a sufficiently large alkali feldspar isolation. From sample V-1, three separate isolations were made (V-1 no. 1, no. 2 and no. 3) one of which was split to make a duplicate (giving rise to V-1 no. 1, (I) and (II)). From V-7, separate isolations were made of a very pure white alkali feldspar (V-7 White) and from alkali feldspar stained brick-red by allanite radio-activity. From the other three samples TT-1, TT-2 and V-2, only one alkali feldspar separation was made.

The nine alkali feldspar samples, accompanied by two duplicated standards, NBS alkali feldspar standard 70a, and G.S.A. granite standard G-2, were subjected to a

routine atomic absorption dissolution and dilution procedure. They were then analysed for barium, calcium, sodium and potassium, the results of which are tabulated below (Table 6).

### Data

Table 6 presents the results of the atomic absorption study. An estimate of the accuracy of the data can be made by assuming that the data for all four elements are equally accurate. Then from the four analyses made by the author of the two standards used in the study, a total of fourteen comparisons can be made to the accepted analyses of the standards (two for each of the three elements analysed in Standard 70a, and two for each of the four elements analysed in Standard G-2). Then from the disparities between the accepted analysis of each standard, (labelled "Std 70a (NBS)", and "Std G-2 (GSA)" in Table 4), and the author's standard analyses, the relative standard error can be computed to be 6 percent. If this statistic is accurate, then 95 percent of the data should be correct to within  $\pm 15$  percent of the amount present. The disparity of 17 percent (of the average value) between the two Ba analyses of V-1 no. 1, though large, is not statisti-

Table 6: Results of Atomic Absorption Spectroscopy: -K-feldspar Old Chelsea Outcrop

SAMPLE NO.	WT.% Ba	WT.% BaO	WT.% CELSIAN	WT.% Ca	WT.% CaO	WT.% ANORTHITE	WT.% Na	WT.% Na <sub>2</sub> O	WT.% ALBITE	WT.% K	WT.% K <sub>2</sub> O	WT.% ORTHOCLASE
Std 70a (I)	---	---	--	0.08	0.12	0.58	1.88	2.53	21.4	8.92	10.74	63.6
Std 70a (II)	---	---	--	0.09	0.12	0.61	1.96	2.64	22.4	9.46	11.39	67.4
Std 70a (NBS)	---	---	--	--	0.11	0.55	--	2.55	21.6	--	11.8	69.8
Std G-2 (I)	0.172	0.192	0.47	1.27	1.78	8.81	3.04	4.10	34.7	3.73	4.49	26.6
Std G-2 (II)	0.181	0.202	0.49	1.34	1.88	9.43	3.13	4.22	35.7	3.85	4.63	27.4
Std G-2 (GSA)	---	0.20	0.49	--	1.97	9.94	--	4.10	34.7	--	4.46	26.4
LL-2	0.162	0.182	0.44	0.27	0.38	1.90	1.22	1.65	14.0	9.43	11.38	67.3
TT-2	0.040	0.045	0.11	---	---	---	---	---	---	---	---	---
TT-3	0.054	0.060	0.15	0.33	0.47	2.31	1.32	1.78	15.1	8.90	10.71	63.4
V-1 #1 (I)	0.144	0.161	0.39	0.30	0.43	2.11	1.19	1.61	13.6	9.49	11.43	67.7
V-1 #1 (II)	0.169	0.189	0.46	0.29	0.41	2.04	1.27	1.71	14.5	10.3	12.45	73.7
V-1 #2	0.151	0.169	0.42	0.52	0.73	3.60	1.77	2.38	20.2	9.03	10.87	64.4
V-1 #3	---	---	--	0.50	0.70	3.47	1.64	2.20	18.7	9.94	11.96	70.9
V-2	0.186	0.208	0.51	0.93	1.30	6.43	1.96	2.64	22.4	7.45	8.98	53.1
V-7 Red	0.124	0.139	0.30	0.32	0.44	2.19	1.93	2.61	22.1	9.68	11.66	69.1
V-7 White	0.124	0.139	0.30	---	---	---	---	---	---	---	---	---

cally significant. All other comparable data are within 9 relative percent of each other.

#### Discussion of Data

From Table 6 the barium content of the analysed feldspars, ranging from 0.04 percent to 0.19 percent by weight is lower than an average value for microcline (from 44 analyses, Smith, 1974, Vol 2, p. 38) of 0.23 weight percent. However the Ba content of alkali feldspars varies within such wide limits (from 43 p.p.m. to 0.95 percent by weight in the published analyses examined) that the above disparity is hardly bizarre. More compelling is the variation within the suite of analyses. Even ignoring the nonconsanguineous V-2 and V-7, the Ba content in the suite of analyses varies by a factor greater than four, variation which far exceeds experimental uncertainty. The scale of this inhomogeneity is of course not determinable, but from the sample distribution alone, it must manifest itself on a scale smaller than 5 meters.

Also evident from Table 6 is the variation in sodium content of the feldspars. The variation within

the three V-1 isolations is sufficiently large to be outside of experimental error at the 95 percent confidence level. However it is not possible to determine the extent to which this variation may be caused by plagioclase contamination. The percentages of sodium listed in Table 6 are therefore maximum figures.

Finally, from Table 6, the average barium content of V-1 and the typical granodiorite samples is 0.11 weight percent, or 0.3 mole percent celsian. If celsian dissolves in alkali feldspar at these concentrations without deviation from Raoult's Law, the dissolved celsian in the analysed feldspars would elevate the refringence of alkali feldspar by an amount equivalent to one mole percent albite. Thus it is unlikely that barium made an important contribution to the disparity between the microprobe analyses of alkali feldspar and the immersion oils results.

## SYNTHESIS OF ANALYTICAL RESULTS

Let us now compare the atomic absorption analyses to those of the electron microprobe. From this some general conclusions can be made concerning both the consistency of the two analytical techniques and the composition of the feldspars in the study areas.

First it is evident that the atomic absorption analyses corroborate the variability in alkali feldspar composition implied by the microprobe analyses. The sodium content in V-1 varies from 14.1 percent\* albite (average of two V-1 no. 1 analyses) to 20.2 percent even though alkali feldspar separations from V-1 were the easiest to make and are therefore the least contaminated with plagioclase. Significant variation is also found in barium content in the atomic absorption analyses. This further supports the concept of inhomogeneous alkali feldspar in the Old Chelsea outcrop.

Sodium and calcium contents indicated by the atomic absorption analyses in general are somewhat lower than the

---

\* Weight, molar and volume percentages will hereinafter be used interchangeably, as the differences between the three quantities are negligible compared to the error implicit in measuring them.

alkali feldspar host phase analyses made on the microprobe, if one takes into account the large amount of exsolved plagioclase in most alkali feldspar crystals of the Old Chelsea outcrop.

The atomic absorption analyses indicate an average of 17 percent albite and 3 percent anorthite in the alkali feldspar. The microprobe analyses average 9 percent albite. In addition point count surveys (presented in a later chapter) indicate an average of 17 percent exsolved plagioclase, though this varies widely from under 5 to over 30 percent. Furthermore microprobe analyses (PC-83, PC-89, discussed below) indicate that a large fraction of these plagioclase lamellae are andesine, approximately 33 percent anorthite. If all the exsolved plagioclase lamellae are andesine as seems to be the case (p.112), the lamellae would be equivalent to 12 percent albite in the alkali feldspars. This, in conjunction with the host phase albite constitutes an independent estimate of 21 percent albite in the alkali feldspar. Though, from the microprobe analyses, there is almost no calcium in the host phase of the alkali feldspar, the andesine lamellae would contribute 6 percent anorthite to the whole alkali feldspar.

The atomic absorption analyses are lower both in sodium and in calcium than this independent estimate. Though it is difficult to determine whether the disparity between these two estimates is significant, in light of the variability in exsolved plagioclase modes, the disparity may indicate that the author's point-counted estimates of modes of exsolved plagioclase lamellae are too high. This overestimate is quite possible, as many of the plagioclase lamellae are quite small and do not extend the full thickness of the section. In this case only those lamellae extending to the surface of the section should be counted, yet at times it is very difficult to resolve the "depth" at which a lamella is seated. All such "moot points" were counted, and may have somewhat magnified the author's mode estimates. Thus the author's exsolved plagioclase modes are maximum figures.

It is important that the sodium and calcium contents indicated by the atomic absorption analyses are also maximum figures due to the probability of a small amount of plagioclase contamination. The large amount of anorthite (over 6 percent) in the analysis of V-2 for example, is excessive, as there is neither sufficient calcium in the microprobe analyses, nor exsolved andesine as indicated by the mode counts, to explain it.

## PETROGRAPHY: OLD CHELSEA OUTCROP

### General Texture and Mineralogy

It is useful to launch the following petrographic study of the Old Chelsea outcrop from a modal analyses of its mineralogy. The results of such an analysis are presented in Table 7. It is also useful for petrographic purposes to compare the typical granodiorite samples, the gneiss variants, and the nonconsanguineous rocks.

There now follows a description of the modal variations of the minerals in samples of the host granodiorite, as presented in Table 7. Immediately evident is the striking variation in the modes of minerals present. For example, the alkali feldspar content of the typical host granodiorite ranges from 7 percent to 31 percent and this variability is very local. The extremes quoted above are from TT-2 and TT-3, respectively, which are separated by a distance of only six inches. The modes of the variant granodiorite specimens are embarrassingly less variable (alkali feldspar ranges only between 10 percent and 17 percent) than those of the typical granodiorite, which were chosen for their apparent homogeneity in hand specimen. Comparable variations are shown with respect

Table 7: Old Chelsea Outcrop: Bulk Mineral Modes

Sample No.	Alteration Minerals	Biotite	Albite (Expelled)	Hornblende	Plagioclase	Chlorite	Quartz	Opaque	K-feldspar	Carbonate	Points Counted
TT-1	3.5	1.5	1.8	11.6	30.5	1.2	23.1	0.6	25.1	0	980
TT-2	0.6	1.0	1.0	5.2	42.3	0.3	16.2	0.4	31.4	0	969
TT-3	2.2	2.6	2.1	8.2	61.0	3.3	13.8	1.5	6.7	0	939
LR-1	3.9	3.3	2.3	2.5	31.2	12.8	28.5	1.2	14.1	0.1	1000
LR-2	2.0	3.7	3.5	2.9	32.5	13.1	13.9	1.7	26.6	0.3	1000
LL-3	1.0	2.7	2.1	2.4	39.9	16.0	15.1	0.4	20.5	0	1000
LL-4	1.3	4.1	1.6	5.2	40.2	3.1	18.1	0.6	25.7	0.1	1000
V-1	0.4	2.7	1.9	6.6	45.7	1.7	23.7	0.3	17.0	0	1000
V-2	1.0	1.1	3.0	0.8	38.6	0.8	30.6	2.4	19.6	0	500
V-3	0.6	0	2.8	0	54.0	12.3	19.2	1.4	9.8	0	1000
V-5	0.9	1.2	1.0	3.1	51.3	6.4	22.4	0.4	12.6	0.7	1000
V-6	0	1.8	2.7	2.1	52.9	8.5	17.5	2.7	11.4	0.4	1000
V-7	1.2	0	2.4	0	13.8	2.1	25.0	0.8	54.6	0.1	746

Modes of V-2 ignore 2 percent tourmaline.

Values for each mineral are in percent.

to quartz and plagioclase. Quartz varies between 14 percent and 29 percent in typical specimens and between 18 percent and 24 percent in the variants. Plagioclase ranges from 31 percent to 61 percent of the typical granodiorite specimens and from 46 percent to 54 percent in the variant samples. Other minerals show similar variations. Notable are the "alteration minerals", ranging from 1 percent to 17 percent of the typical samples. The variability in mineral modes throughout the Old Chelsea suite of specimens has important geothermometric ramifications, as will be pointed out later.

The modes of the two nonconsanguineous samples are also presented in Table 7. V-2 is lower in biotite and hornblende (3 percent total versus 10 percent) than the average of the typical host specimens, but is higher in opaques (2 percent versus 1 percent) and quartz (30 percent versus 18 percent). Tourmaline is present as approximately 1 percent of the rock. From Table 7, V-7 can be seen to be nearly devoid of mafic minerals, but higher in quartz (25 percent versus 18 percent) than the average of the typical host specimens and much higher in alkali feldspar (55 percent versus 21 percent). V-1 is more felsic than the average of the typical host specimens (87 percent versus 79 percent) with more quartz (24 percent

versus 18 percent) being present. These differences are rather slight, but may reflect the locally derived pegmatitic origin of V-1. V-3 is much higher in alteration minerals than the typical host granodiorite (13 percent versus 9 percent). Content of alteration minerals varies greatly in both typical and variant granodiorite samples, and reflects inhomogeneity in the degree of alteration. Though retrograde metamorphism has been locally severe, it has not been penetrative. V-5 and V-6 display only insignificant or fortuitous modal variations. The modal mineralogy of V-6 shows no sign of metasomatic effects from V-7.

#### Classification of Rock Types in Old Chelsea Outcrop

The wide variations in modal mineralogy expressed in the suite of Old Chelsea specimens reflects itself in the classification of these rocks. To show this variability, the bulk mineralogy of each specimen in the suite is plotted in Figure 9 according to Streckheisen's (1967) classification. From Figure 9, rock compositions within the host gneiss vary from near the quartz diorite field to quartz-rich granodiorite to quartz-bearing monzonite, with the average composition being a quartz-poor granodiorite. The average composition would fall within Hogarth's

(1970) map unit 8b (p. 20), roughly intermediate between the compositional extremes shown by the Old Chelsea mass (p. 20). The tourmaline pegmatite, V-2, is seen to be surprisingly plagioclase-rich. However, the author chose the thin section in an unrepresentatively fine grained portion of the sample and most of the alkali feldspar in the sample is very coarse grained. Perhaps alkali feldspar is unrepresentatively scarce in the thin section. V-7 is seen (Fig. 9) to be a potash-rich granite.

#### General Texture

This section presents an overall view of the texture of the rock of the outcrop as a whole. More detail is given in the individual mineral descriptions.

The host granodiorite is in general medium grained and even grained. Grain size averages about 1.5 mm and varies continuously, with 90 percent of grains between 0.2 mm and 3 mm. Grain shape is in general anhedral and equant. Some grains are polygonal with near-120° triple junctions. Grain boundaries tend to be smooth and simple, showing relatively little surface area per unit volume. The textural properties of the host granodiorite imply a history of some recrystallization of the primary igneous fabric

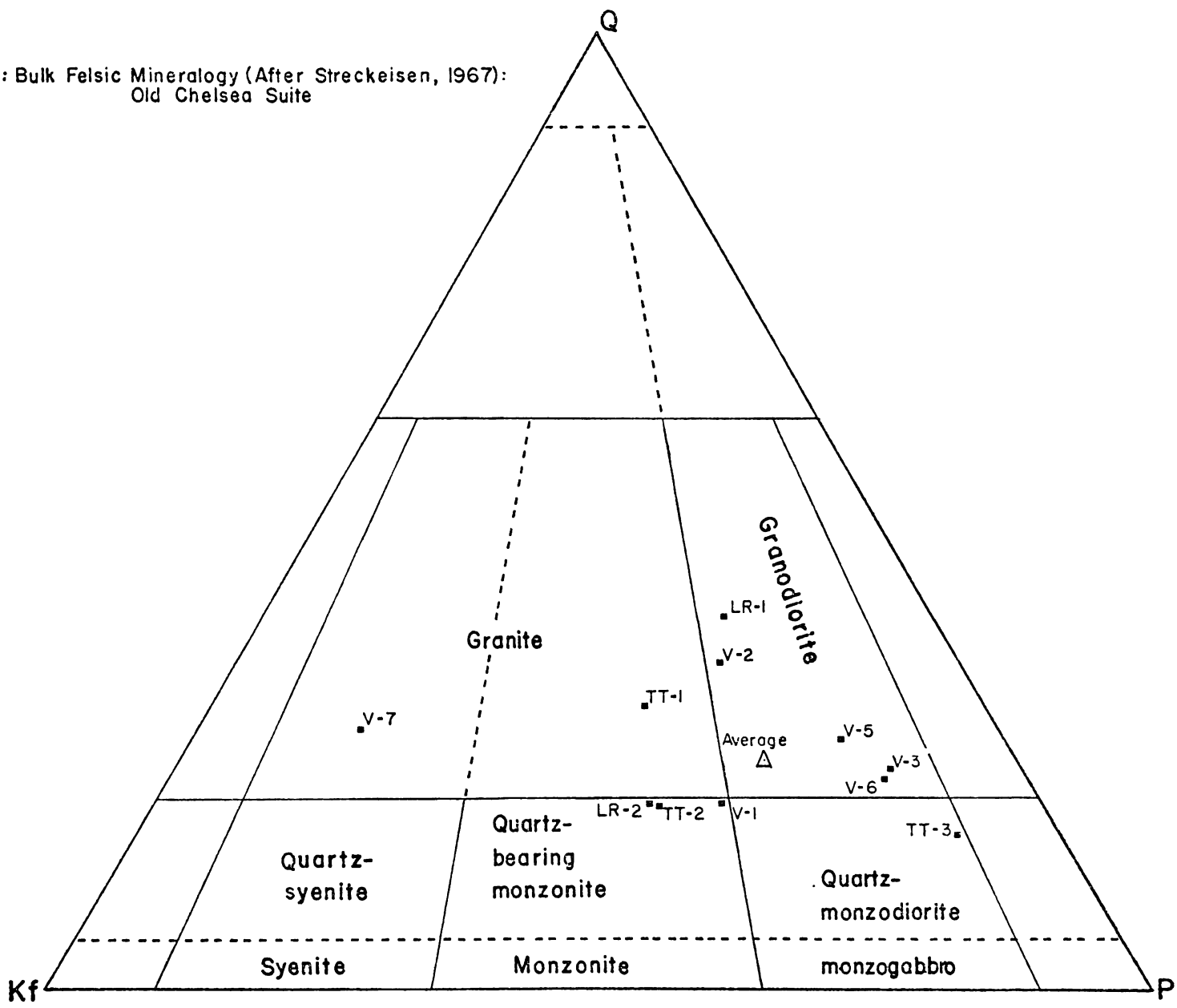
under solid state metamorphic conditions. This recrystallization process is not extensive however, and the rock retains some elements of its primitive igneous texture (see the mineral descriptions, below).

Gneissosity is very weak but, on the scale of the whole outcrop, is penetrative. However, the rock is not visibly gneissose in thin section. The weakness of the gneissosity is probably due to the relative scarcity of mafic minerals (notably biotite), in combination with the low intensity of prograde metamorphic recrystallization. The only metamorphic fabric visible in thin section is retrograde. It is local, and, even on the scale of the whole outcrop, is non-penetrative, but it shows particularly well in LR-1 and LR-2. It expresses itself as a set of sub-parallel, planar, tabular zones of concentrated alteration minerals. These alteration zones occupy small cracks in the rock which invade and fracture crystals of primary minerals. Alteration of the primary minerals is not enhanced near these zones.

The tourmaline pegmatite represented by V-2 is medium grained but not equigranular, with average grain size varying from 2 mm to 4 mm. Grain size varies continuously. 90 percent of mineral grains are between

Figure 9: Classification of Old Chelsea outcrop samples after Streckeisen, 1971, as inferred from point-counted bulk mineral modes (Table 7). Average compositions does not include V-2 and V-7.

Figure 9: Bulk Felsic Mineralogy (After Streckeisen, 1967):  
Old Chelsea Suite



23

(85)

0.05 mm and 10 mm in diameter. The feldspars give the rock a generally subhedral grain shape. Some crystals of both plagioclase and alkali feldspar are lathlike, not equant. Grain boundaries are more irregular than in the host gneiss, with a larger proportion of crystals invading and including each other. V-2 has a more typically igneous texture, with no evidence of recrystallization in the solid state.

The nonconsanguineous aplite of V-7 is less distinct texturally from the host granodiorite, but is finer grained, averaging 1 mm, and shows less variation in grain size, with most grains between 0.2 mm and 1.5 mm in diameter.

#### Descriptive Mineralogy

The following mineral descriptions are applicable to the host gneiss unless it is stated otherwise. Modes, having been treated in detail above, will not be considered.

Alkali feldspar occurs as anhedral grains, only very slightly elongated along the c-axis. Grains average about 2 mm in diameter, slightly above the average for the whole rock. Distribution is not random, instead alkali feldspar crystals tend to occur in "clumps" of four to ten, isolated

from other aggregates. The extreme modal variation of alkali feldspar between closely spaced thin sections (eg. TT-2, -2 and -3) is a manifestation of the same phenomenon on a slightly larger scale. Small aggregates may have resulted from granulation of larger crystals. Alkali feldspar is intimately and obligately associated with myrmekite in plagioclase. This is dealt with in greater detail in a subsequent chapter.

Crystallographically, the alkali feldspar is microcline. It is optically negative, with  $2V$  estimated from a centered optic axis figure, as  $75^\circ \pm 10^\circ$ . This figure for an alkali feldspar containing roughly 9 percent albite corresponds to an Al/Si disorder of about 85 percent  $\pm 15$  percent (Stewart, 1974), reasonably close to maximum microcline. Twinning is very fine and nearly ubiquitous on both the albite and pericline laws, generating the familiar "tartan" effect.

The alkali feldspar in the Old Chelsea outcrop demonstrates an optical crystallographic anomaly which was at first confusing. It was discovered that  $010$  cleavage fragments in oil mount always gave a perfectly centered obtuse bisectrix figure. This belies the feldspar's known triclinic nature, as ordered alkali

feldspar is known to have an angle between crystallographic  $b^*$  and optic  $\mathcal{V}$  of  $18^\sim$  (Deer, Howie and Zussman, 1966). The apparent coincidence of  $b^*$  and  $\mathcal{V}$  in the Old Chelsea alkali feldspars is believed to be due to the very fine twinning. The close proximity of inverted crystal structures generated by the twinning acts to cancel out the obliquity of  $b^*$  to  $\mathcal{V}$ .

The chemical composition of the alkali feldspar will be discussed below. Exsolved plagioclase will also be dealt with in a later chapter.

Plagioclase occurs as equant anhedral crystals averaging, like alkali feldspar, 2 mm in diameter. The crystals are not exemplary of lathlike igneous feldspars. The most common irregularities in a dominantly smooth, simple crystal outline are myrmekitic excrescences occurring where plagioclase crystals border on alkali feldspar. This textural feature will be discussed below. Plagioclase is dispersed throughout the rock in a random manner, having no strong affiliations with other minerals.

Plagioclase in the Old Chelsea granodiorite has a high negative  $2V$  ( $2V_\alpha = 85^\circ$ ) and is therefore in the low albite series, which is congruent with the feldspar's

metamorphosed plutonic paragenesis. Most plagioclase in the outcrop is uniformly andesine, averaging 35 mole percent anorthite, but normal zoning of about 3 mole percent anorthite is present in a narrow rim around some crystals. In addition, the andesine crystal cores have optically discontinuous rims, usually narrower than 0.2 mm, of low calcium plagioclase. Though microprobe data on their composition is lacking, optical data indicate an anorthite content of 0 to 10 mole percent. Thus they can correctly be called albite rims. Albite is the only plagioclase present in V-2 and V-7, and in the highly altered gneiss variant V-3, albite is the only unaltered plagioclase, the andesine having been completely saussuritized. Lamellar twinning is common in the plagioclase with the Albite Law preponderating. Pericline twins intersect the albite twins on some crystals and in a few crystals actually dominate the albite twins. Carlsbad twinning is absent.

Quartz occurs as anhedral grains averaging 2 mm in diameter. Quartz grains are more irregular in shape than those of feldspar, less consistently equant and with more deeply embayed, convoluted grain boundaries. Quartz

occurs as aggregates like alkali feldspar, though perhaps to a lesser degree. Quartz crystals include tiny rutile needles and quartz occurs symplectitically with plagioclase as myrmekite. Quartz also occurs with hornblende, biotite, carbonate and opaque minerals in the symplectite discussed in the description of hornblende. Quartz has section extinction, presumably due to strain. All plates in a single crystal come to extinction within a range of  $5^\circ$  of rotation.

Hornblende is in general finer grained than the felsic minerals, averaging 0.5 mm but grain size is extremely variable with 90 percent of grains between 0.04 and 2.5 mm in diameter. Hornblende grains are anhedral to subhedral, with some elongation parallel to the c-axis. Amphibole is the most strongly aggregated mineral in the suite. The amphibole clots range in size and complexity from small aggregates of three or four 0.5 mm amphibole crystals to symplectitic complexes 4 mm in diameter which are obviously pseudomorphic after a former large crystal. The mafic symplectite is best developed in TT-1 and consists of amphibole, quartz, carbonate, biotite, opaque minerals and occasional sphene

and epidote. A fully developed symplectite has three zones. At the core is an embayed crystal of common hornblende, poikiloblastic with quartz and carbonate and altering patchily to tremolite. Surrounding this is an intermediate band of very small hornblende grains. These are very poikiloblastic and strongly embayed by quartz, occasionally so severely that the hornblende exists as wormlike grains intercalated with quartz. Most of the biotite, opaque minerals, and carbonate occurs here. The exterior zone is of densely packed, equant 0.5 mm grains of ferrohastingsite, some of which have minor wormy penetrations of quartz. In the vicinity of the mafic symplectite there is often some satellitic biotite and carbonate. The extinction of the amphibole grains is fairly coherent in the best developed mafic symplectites. The majority of crystals go to extinction within a few degrees of rotation, and the overall effect is of compositional zonation from core to rim. These mafic symplectites are the results of a retrograde metamorphic reaction involving an earlier, higher temperature mafic silicate, the precise nature of which is not certain. What can be inferred from this symplectite will be discussed later. Amphibole occurs intimately with chlorite along cleavage planes. Where

chlorite is abundant, small amounts of opaque oxide occur in the chlorite as wormy grains.

Optical evidence indicates three varieties of amphibole in the Old Chelsea granodiorite. Most abundant is a common hornblende, pleochroic from pale olive to blue-green. It is simply twinned with an hk0 composition plane and has an anomalous blue-green extinction in low birefringence orientations. The amphibole has  $2V_{\alpha} = 70^{\circ} \pm 10^{\circ}$  and  $Z \wedge C = 24.5^{\circ}$ . A much paler amphibole, pleochroic colourless to pale blue-green occurs as optically continuous patches within the common hornblende, and its composition is inferred to be at or near that of tremolite. The third variety of amphibole has an intense blue-green body colour with a negative 2V of only about  $20^{\circ}$ . It has a low birefringence and an anomalous green extinction due to its body colour. Its composition is inferred to be at or near that of ferrohastingsite.

Biotite in the host granodiorite has on the average a larger and less variable grain size than hornblende, averaging 0.75 mm in diameter. Grains lack side terminations and have numerous inclusions of zircon and quartz. Biotite occurs in association with the mafic symplectite

but is not confined to it. It is pleochroic from green to green-brown and 2V is quite small, only about 5°.

The opaque minerals occur as anhedral 0.3 mm grains, Pyrite predominates and occurs as the largest grains. Magnetite and hematite also occur in obligate association with each other. Pyrite shows a very strong association with the oxide minerals and forms the core of well developed aggregates, rimmed by the oxide minerals. Under high magnification the oxide rim can be seen to consist of a magnetite core completely surrounded by hematite, with pyrite and hematite in contact. This has probably resulted from the oxidation of pyrite under variable pO<sub>2</sub> conditions, although pyrite and hematite can form at equilibrium under oxidizing conditions where the amount of dissolved sulfur remains high (Krauskopf, 1967, p. 253).

Two chlorite minerals occur in the Old Chelsea outcrop. The most abundant chlorite is dull green and optically negative (length slow), with anomalous "Berlin Blue" extinction and a maximum birefringence of approximately 0.010. It occurs as felted masses of tiny anhedral grains along cleavage planes in hornblende and biotite, and with serpentine in tabular alteration zones. In addition there

are a few euhedral sheafs of chlorite which are pleochroic colourless to pale blue-green, with anomalous brown extinction and low birefringence. The sheafs are 0.1 mm in diameter and occur near masses of the other chlorite.

Serpentine occurs in tabular alteration zones and in a few samples as equant masses with poorly formed "hourglass" extinction.

Two epidote group minerals occur in the study outcrop. True epidote occurs as equant anhedral crystals about 0.3 mm in diameter. Birefringence is greater than 0.40 and pistachio-green pleochroism is evident. Epidote is associated with the mafic symplectite, closely allied with carbonate. A second epidote mineral occurs as saussurite in plagioclase. The acicular crystals have an extinction angle of less than 5° and a birefringence of about 0.10. The mineral is probably clinozoisite.

White mica also occurs in small amounts in saussurite. Its modes are pooled in Table 7 with those of epidote and serpentine, under the heading of "Alteration Minerals".

Both sphene and zircon occur in small quantities in the Old Chelsea outcrop. Sphene rims pyrite and magnetite.

Zircon occurs as very small grains in chlorite and biotite. Carbonate also occurs, especially in the mafic symplectite. Acicular apatite crystals are scattered inclusions, mostly in the felsic minerals. Rutile is common in quartz as very fine needles. A dark green variety of tourmaline occurs in V-2 as stubby equant crystals up to 1 cm in diameter.

#### Alteration of the Old Chelsea Granodiorite

The complete mineral assemblage of the typical granodiorite could not have formed in equilibrium with a single pressure and temperature. Instead the maximum prograde mineral assemblage of hornblende-biotite-andesine-perthite-quartz pyrite has been modified by several alteration reactions. The reactions altering plagioclase to saussurite and biotite to chlorite are obvious. However the lack of analytical data on the mafic, accessory, and alteration minerals prevents deduction of the mechanisms of these and other alteration reactions.

Especially troublesome are the reactions generating the mafic symplectite, as not even the reactant mineral is known for certain. Judging from the high calcium,

aluminium, iron and magnesium content of the product minerals, the reactant phase would almost certainly have been either an amphibole or a pyroxene. However pyroxene is nowhere evident, and the common hornblende cores of the symplectite with their strongly embayed margins and in situ alteration to tremolite show strong textural evidence of being the reactant phase of the symplectite. The product minerals include at least two amphiboles. One is near the composition of ferrohastingsite, and another is near that of tremolite, with a third amphibole, common hornblende, possibly at or near the composition of the original reactant mineral. Other products must be quartz, carbonate and pyrite, with biotite, magnetite, and epidote very likely as well.

The mineralogy of the alteration products, together with the textures in the symplectite (as described above) indicate retrograde breakdown of a higher grade, possibly more tschermakitic, hornblende to lower grade amphiboles.

An attempt has been made to quantify the extent of greenschist-facies alteration in the Old Chelsea samples. The method used for each specimen was to sum the modal percentages (Table 7) of hornblende, biotite, the opaque

minerals, chlorite, and the "alteration minerals" (mainly serpentine and epidote, including some saussurite). This figure was divided into the sum of the modes of chlorite and the "alteration minerals". The result is expressed as a decimal fraction and is referred to as the "degree of alteration" of a sample.

This "degree of alteration" criterion may be inconsistent for at least two reasons. First, the small amount of saussurite in the "alteration minerals" column of Table 7 has altered from plagioclase rather than a mafic mineral, and some of the epidote may have had a similar origin. Second, processes of secondary alteration involve subtle chemical changes as well as changes in mineralogy, and hence alteration probably cannot be petrographically evaluated with great accuracy. However, the approach used is a useful simplification of a complex problem.

From the viewpoint of the criterion used, specimens LR-1, LR-2 and LL-3 would be described as severely altered, and V-3 is the most severely altered specimen in the suite. TT-2 has been the least subject to retrograde metamorphism and V-1 is also not badly altered.

The remainder of samples are intermediate between these extremes, including V-5, which appears exceptionally fresh in the outcrop. The degree of alteration of some Old Chelsea specimens is shown in Figure 11.

Let us now focus on the distribution of a secondary alteration mineral of particular interest. In Figure 10, the mode of albite (expressed as percentage of plagioclase\*) is plotted against the percentage of the nearby rock that is alkali feldspar. The data were acquired during detailed point counts of small portions of the thin sections (with areas averaging about 25 mm<sup>2</sup>), and are fully presented in Table 9. Note in Figure 10 that despite the anomalous point acquired from a portion of LR-1, there is a distinct correlation between the thickness of albite rims on plagioclase and the amount of nearby alkali feldspar. This correlation implies that albite presently rimming plagioclase is somehow linked to alkali feldspar.

From the modes in Table 7 was prepared Figure 11,

---

\* The "Others" column of Table 9 is deemed, for the purposes of Figure 11, to be a sufficiently consistent approximation of plagioclase modes.

Figure 10: Thickness of albite rims on plagioclase in Old Chelsea outcrop samples, as related to the abundance of nearby perthitic alkali feldspar. Data were acquired from detailed point counts presented in Table 9.

Figure 10: Correlation Of Albite Rims On Plagioclase To Nearby K-feldspar



001

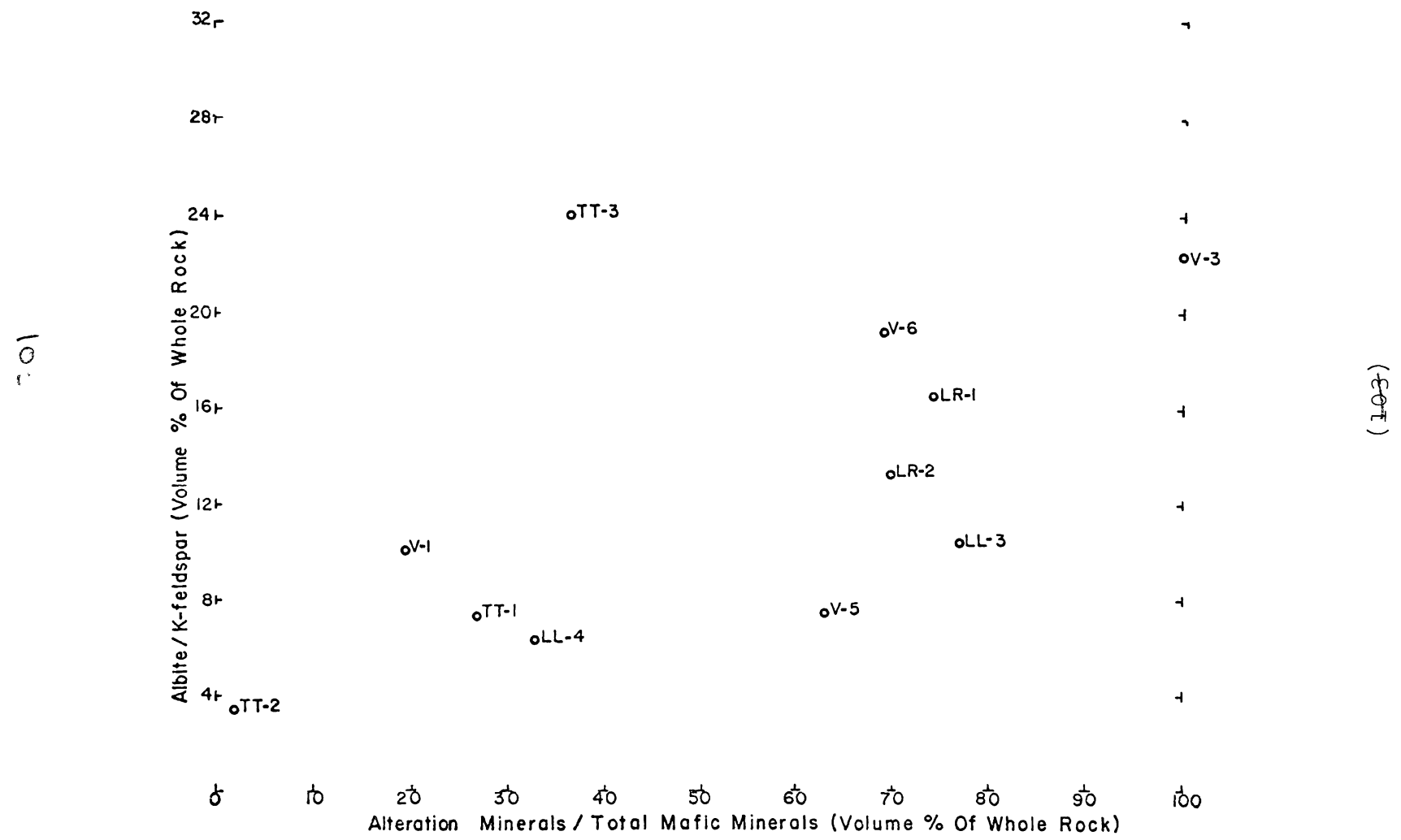
(001)

which shows the relationship between the degree of alteration in a sample and the amount of albite present. Since albite is linked to alkali feldspar (Figure 10), the albite modes in Figure 11 were divided by the sum of the modes of albite and alkali feldspar. The correlation in Figure 11 is not as clear as that in Figure 10 and the point for TT-3 is anomalous. However, some of the scatter in Figure 11 may result from the difficulty in ascribing an internally consistent "degree of alteration" factor to the samples. In any case, despite its inadequacies, the graph demonstrates a correlation between albite modes and greenschist-facies alteration.

A further observation can be made concerning the distribution in the host granodiorite of albite and of plagioclase exsolved from alkali feldspar. In Figure 12 the amount of albite rimming plus the amount of exsolved plagioclase lamellae (taken from Table 9 and expressed as a volume percentage of the sum of the modes of albite and perthite) in the microprobe target area of each sample is plotted against the contents of the microprobe analyses for each sample. The

Figure 11: Albite: alkali feldspar ratio (p.101) in Old Chelsea outcrop specimens showing a range in the degree to alteration of hornblende and biotite to chlorite, epidote and serpentine. Data were acquired from bulk mineral point counts, presented in Table 7.

Figure 11: Correlation Of Albite Rims On Plagioclase To Degree Of Alteration

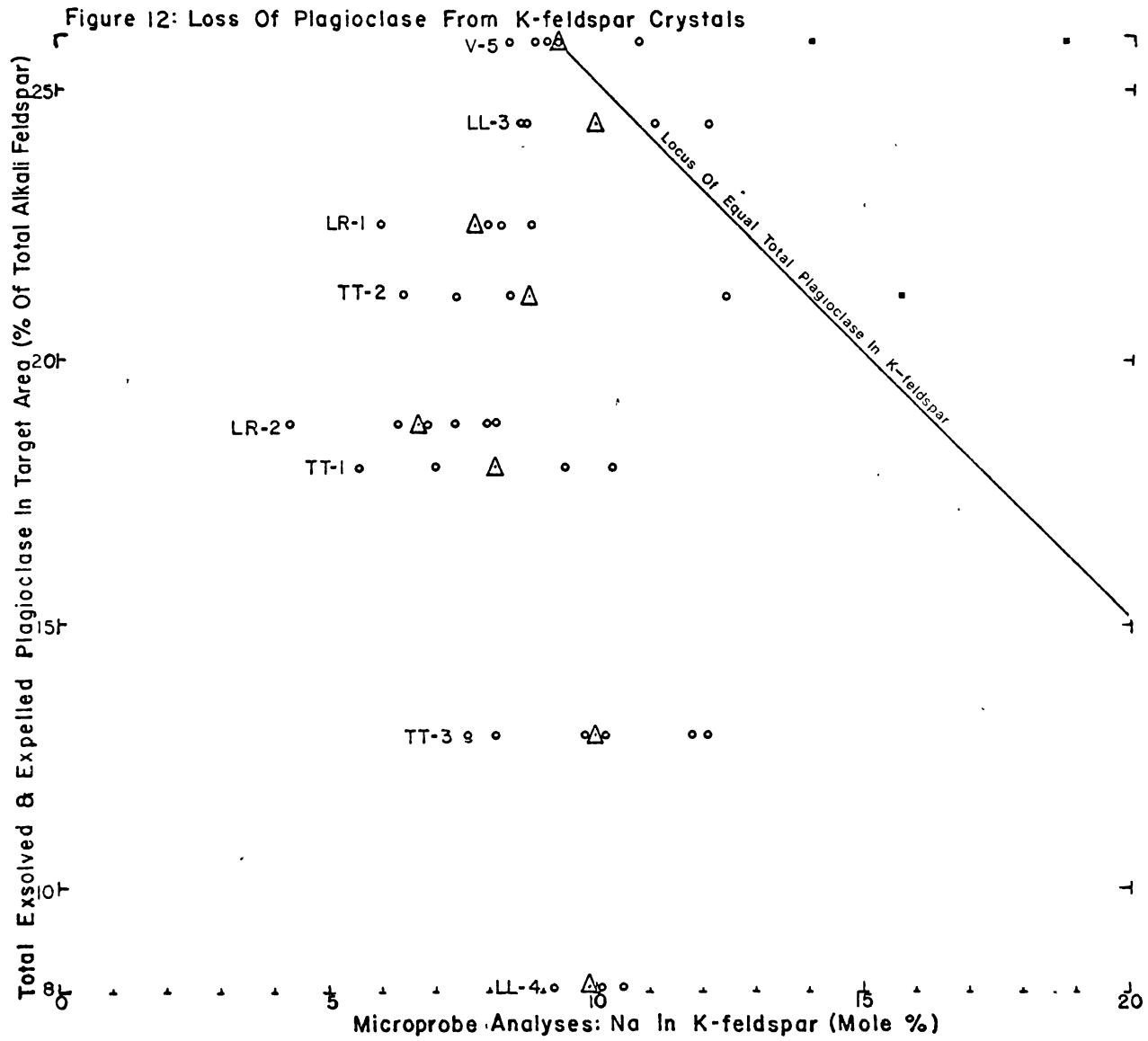


average sodium content of the microprobe analyses for each sample is represented as a triangular point. The solid line of negative slope in Figure 12 is the locus of alkali feldspars showing varying degrees of plagioclase exsolution but all having the same bulk composition with respect to sodium as the estimated average for sample V-5.

Figure 12 demonstrates that alteration does not affect the total amount of sodium in or near the alkali feldspar microprobe target crystals. For example, the samples with the highest content of formerly dissolved plagioclase in or near the target alkali feldspar crystals are V-5 and LL-3, which are moderately altered (Figure 11). TT-2, the freshest specimen, has less of this plagioclase than the two moderately altered samples.

The variation in total Na-content between samples (and indeed within samples) has a further significance. If equilibrium between the crystallizing plagioclase and alkali feldspar in the Old Chelsea outcrop was ever achieved, the total plagioclase content of alkali feldspar would have been constant throughout the outcrop. Now, the identical composition of exsolved plagioclase lamellae and of external plagioclase crystals (p.112)

Figure 12: Plot of the total plagioclase within, or believed to have originated from, alkali feldspar, as compared to the amount of dissolved sodium remaining in the alkali feldspar, as disclosed by the microprobe analyses. Each open circle represents a normal microprobe analysis. Large triangles denote the average of microprobe analyses for each sample. Analyses believed to be overly contaminated with exsolved plagioclase (the "cutoff" was arbitrarily made at 14 percent sodium) are indicated by solid squares, and were not included in the sample averages.



901

(90F)

is potent evidence that equilibrium was in fact maintained at least up to the time of exsolution of plagioclase from the alkali feldspar. Furthermore, there is no textural evidence that sodium has been introduced into the rock of the Old Chelsea samples. It is therefore inescapable that the microprobe target area of LL-4, with a total sodium content of about 18 percent albite has lost about 18 percent more albite to the surrounding rock than has the target area of V-5. Alkali feldspar crystals which are devoid of plagioclase lamellae must have expelled plagioclase originally occupying over 25 percent of their volume.

The synthesis of information from Figures 10, 11, and 12 is as follows. The amount of albite rimming plagioclase is strongly influenced by the amount of alkali feldspar nearby (Figure 10), which implies that the albite presently rimming plagioclase originated with and was expelled from the alkali feldspar crystals. Since the amount of albite can be independently correlated to the degree of greenschist-facies alteration in the rock (Figure 11), it is logical that the precipitation of albite onto the plagioclase crystals was

one of the processes operant during this alteration.

Now, it is known (Table 8) that the modes of exsolved plagioclase in alkali feldspar crystals are extremely variable and unrelated to the amount of plagioclase still dissolved in the alkali feldspar (Figure 12). Thus there are differences from one small area to another in the total plagioclase component remaining in the alkali feldspar crystals and these differences cannot be eliminated by including the modes of albite nearby.

Figures 10 and 11 combine to indicate that albite expelled during low grade alteration did not leave the immediate vicinity of its expulsion. Hence the variability in composition which now exists must have been initiated at some higher grade than greenschist facies, which in turn requires that the plagioclase expulsion process was initiated at this higher grade. The expulsion process then either continued while metamorphic conditions gradually shifted into the greenschist facies, or was again activated during a later greenschist overprint.

## EXSOLVED FELDSPAR: OLD CHELSEA OUTCROP

### Alkali Feldspar Exsolved from Plagioclase

Antiperthitic plagioclase is very rare in the host granodiorite of the study outcrop, though one plagioclase crystal with 5 percent exsolved alkali feldspar was observed in TT-1. In the tourmaline pegmatite (V-2) however, many of the lathlike, igneous feldspar crystals are antiperthitic (Plate 3A). The exsolved alkali feldspar is "tartan" twinned and occurs as angular blocks up to 0.5 mm in diameter. The exsolved alkali feldspar in V-2 has been microprobed (analyses KF-133 to -138) and the results indicate that the composition of these lamellae are not different from that of the external alkali feldspar in the pegmatite. This implies that exsolution of alkali feldspar from plagioclase in V-2 occurred in equilibrium with external alkali feldspar.

### Plagioclase Exsolved from Alkali Feldspar

The most salient feature of the plagioclase lamellae exsolved from alkali feldspar is the modal variability. Table 8 shows the modes of exsolved plagioclase in crystals of alkali feldspar which were chosen as microprobe targets or optional targets. Note the variation

Table 8: Modes Of Exsolved Plagioclase In K-feldspar: Old Chelsea

SAMPLE NO.	STATUS OF CRYSTAL	PLAGIOCLASE LAMELLAE (POINTS)	K-FELDSPAR HOST (POINTS)	VOLUME % PLAGIOCLASE IN K-FELDSPAR
TT-1	Microprobe Target	51	225	19
	Optional Target	26	122	18
TT-2	Microprobe Target	36	136	21
	Optional Target	25	121	17
TT-3	Microprobe Target	19	108	15
	Optional Target	10	87	10
	Optional Target	40	140	22
	Optional Target	32	99	24
LR-1	Microprobe Target	14	132	10
	Optional Target	15	94	14
LR-2	Microprobe Target	18	125	13
LL-3	Microprobe Target	46	164	22
LL-4	Microprobe Target	26	120	18
V-1	Probe Target #1	32	197	14
	Probe Target #2	33	156	18
V-2	Microprobe Target	5	135	4
	Optional Target	0	---	0
V-3	Microprobe Target	19	92	17
	Optional Target	5	107	5
V-5	Microprobe Target	47	124	32
V-6	Probe Target #1	17	64	21

within single samples: in TT-3 there are crystals containing 10, 15, 22, and 24 percent exsolved plagioclase. Exsolved plagioclase is ubiquitous in the alkali feldspar of the host granodiorite. Indeed the tourmaline pegmatite (V-2) is the only rock type with very little perthitic alkali feldspar. Exsolved plagioclase lamellae in the study outcrop range in size from large equant blebs 60 microns in diameter, to very fine "stringer" perthite 5 microns in longest dimension, and smaller down to the limits of resolution.

The orientation of the plane of exsolution of plagioclase in the alkali feldspar was observed in several grains in oil mount. For 010 cleavage fragments the angle between the exsolution lamellae and the 001 cleavage (i.e. the trace of the a-axis) is  $75^\circ$ , in good agreement with the angle of  $73^\circ$  for 010 sections given in Deer, Howie and Zussman (1966, p. 292, 295). It is also stated that lamellae are approximately parallel to the b-axis (ibid, p. 292). Since the b-axis of microcline is very nearly perpendicular to 010, the author's  $75^\circ$  measurement is effectively true size. Accepting a  $\beta$  angle of  $115.5^\circ$  for microcline, the plagioclase lamellae lie approximately parallel to 100.

The direction 106 as given in Deer, Howie and Zussman (1966, p. 297) is a good approximation to the attitude of the lamellae.

The composition of the plagioclase lamellae was discovered by probe analyses to be andesine. For example, microprobe analysis PC-83, in sample LL-3, of a lamella indicates that there is 32 mole percent anorthite present. As is the case for alkali feldspar exsolved from plagioclase, the composition of the exsolved plagioclase in alkali feldspar in all samples studied equals that of the external plagioclase grains. Furthermore, this is true both in the Old Chelsea outcrop, and in samples from the Blue Sea Lake area. However, reference to the photomicrograph (Plate 1-A) of the lamella analysed for PC-83 discloses that the analysed lamella is large and equant, in marked textural contrast to the smaller "stringer" type blebs nearby. However petrographic observation in the vicinity of PC-83 reveals that the large, equant lamellae have the same relief in contrast to the alkali feldspar host. This relief contrast is uniformly much higher than that of a nearby albite rim adjoining the alkali feldspar crystal.

Further insight is provided upon examining the vicinity of PC-83 at lower magnification. In Plate 1-B it can be seen that the "stringer" blebs of plagioclase are in zones transected by bands that are low in exsolved plagioclase. It is in these plagioclase-poor bands that one finds the larger more equant blebs such as that of PC-83. Evidence is presented below to prove that these plagioclase-poor zones in alkali feldspar are zones of higher mobility of the exsolved plagioclase, and it is apparent that the larger blebs are not genetically different from the smaller "stringers", but presumably result from the coalescence of the smaller lamellae.

In all thin sections from the Old Chelsea outcrop, all visible exsolved plagioclase lamellae have a uniformly high relief contrast to the alkali feldspar host and are inferred to be andesine. However the microprobe analyses indicate considerable variation in the sodium content of the alkali feldspar host, and that this variation is not accompanied by a consistent proportional variability in calcium content. For example, KF-117, with 19 mole percent sodium, has much less calcium than does KF-120, with only 14 mole percent sodium.

These anomalies perhaps result from imprecision in the performance of the microprobe at the low concentrations of calcium present in the material analysed.

There are other textural peculiarities associated with plagioclase exsolved from alkali feldspar in the Old Chelsea outcrop. Notable are the plagioclase-free rims to most of the alkali feldspar crystals. These rims are from 0.05 to 0.2 mm wide, and are widest where an alkali feldspar crystal juts out into the surrounding rock. Commonly the exsolution lamellae taper off in size and abundance near the rim. There are no optical discontinuities or "ghosts" at these rims; they are not overgrowth features. They are due to expulsion of plagioclase or of plagioclase components from the alkali feldspar crystals, probably either during or after its exsolution from the alkali feldspar host.

In addition, the twinning and extinction in alkali feldspar crystals is not homogeneous but is divided into semi-isolated "domains" with definitely differing modes of exsolved plagioclase. Areas which are sharply "tartan" twinned have high modes of exsolved plagioclase whereas less sharply twinned zones of more undulose extinction

are almost devoid of plagioclase lamellae. Plate 2 shows an example of this "domain" extinction. An example of the untwinned plagioclase-poor domains was microprobed in V-6 (Plate 3B). Analyses KF-121 and -122 demonstrate that the plagioclase-poor zones are not richer in host albite, but in fact may be poorer in it than the plagioclase-rich domains. The unperthitic domains are therefore not areas in which exsolution has failed to take place, but rather, are areas which have lost their plagioclase component through expulsions either to the perthitic domains or to the outside rock. The cause of the crystallographic differences between the two domains is not understood, but it appears that particularly pronounced expulsion has some effect on local crystal structure, or vice versa.

The migration of plagioclase and of dissolved plagioclase components from alkali feldspar crystals has other textural manifestations. Plate 4-B displays a distinct band free of exsolved plagioclase transecting an alkali feldspar crystal. The plagioclase-free band is centered around a crack in the crystal. Note (Plate 4-A) the abundance of albite at the end of the band. Note also

in Plate 4-A that the plagioclase-free band is not sharply twinned. Equally prominent are the roughly conical zones of plagioclase expulsion shown in Plates 6-A and 7-B. The zones are widest at the edge of the crystal, tapering inwards. The plagioclase lamellae are larger and sparser in the expulsion zones, with less exsolved plagioclase overall inside the zones than outside of them. Typically such zones are optically disturbed (Plate 6-A); extinction across the expulsion zone is offset by several degrees with respect to the rest of the crystal. Such zones are, then, another type of "extinction domain". Note particularly how at the edge of the expulsion zone in Plate 7-B, the more elongate lamellae are curving or "wandering" into the zone. This is evidence that the expulsion of plagioclase from the alkali feldspar crystals was occurring at least in part by a process of bulk migration of the plagioclase lamellae through the alkali feldspar lattice, as opposed to a simple process of chemical diffusion. Re-examination of Plate 1-B discloses that the above-mentioned low-plagioclase bands in LL-3 are no different from the plagioclase expulsion zones discussed immediately above.

The obligate association of myrmekite with perthitic

alkali feldspar is well known (Phillips, 1974) but concerning the precise mechanism generating myrmekite there has been some debate (concisely reviewed, *ibid*). Of special interest then is the very strong association of myrmekitic plagioclase with alkali feldspar crystals from which plagioclase expulsion has occurred. This association is demonstrated by the plagioclase expulsion zones in Plates 1-B and 7-B which abut against myrmekitic plagioclase. Similarly, note the well-developed myrmekite near the alkali feldspar crystal in Plate 7-A, where plagioclase expulsion has obviously been extensive. Other textural evidence is the observation that myrmekitic plagioclase in the study outcrop very often occurs as either inclusions in alkali feldspar crystals, or as protuberances (usually more saussuritized than the bulk of the crystal) on the otherwise smooth outline of the plagioclase crystal (Plate 5-B). The former occurrence may result from inclusions of primary feldspar which have subsequently been injected with quartz, but it also exposes the possibility the myrmekite may form when plagioclase exsolves in large quantities from, or in effect locally replaces alkali feldspar. The latter occurrence argues that myrmekite

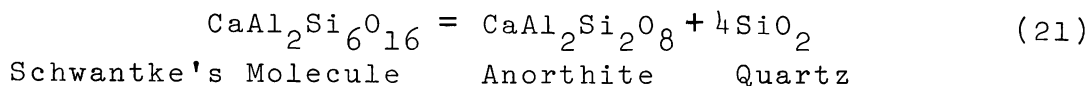
forms as a later overgrowth on existing plagioclase crystals, and possibly argues that it forms under conditions especially conducive to alteration of the newly forming feldspar. A third occurrence of myrmekitic plagioclase (Plate 6-A) is as irregularly shaped, elongate blebs between two alkali feldspar crystals. The habit of these myrmekitic blebs is not consistent with that of the larger, equant plagioclase crystals which are thought to have resulted from mild metamorphic recrystallization of igneous feldspars. The habit of these blebs is more easily explained by their having originated due to the expulsion of plagioclase or plagioclase components from the surrounding alkali feldspar.

A test of the connection between plagioclase expulsion and myrmekite can be made with reference to Figure 12. Recall that at the time of solidification of the Old Chelsea granodiorite, its alkali feldspars must have been homogeneous with respect to dissolved plagioclase. Now, from Figure 12, it is apparent that the samples of the study outcrop have lost heretofore unaccountable and widely varying amounts of plagioclase from the alkali feldspar. Furthermore it is now clear that this plagioclase has been lost through

expulsion from the alkali feldspar crystals. Therefore, if myrmekite is in some way caused by plagioclase expulsion, those samples whose alkali feldspars have lost the largest proportion of their original igneous plagioclase component will contain the most myrmekite. The amount of myrmekite in the samples plotted in Figure 12 does not quantitatively support this hypothesis. For example, myrmekite is roughly equally well developed in samples LL-4 and TT-2, though TT-2 has a higher proportion of its original dissolved plagioclase component than does LL-4. This is at least partially due to the data in Figure 12, which were therefore gathered from small areas of the thin sections, and therefore imperfectly representative of them. Nonetheless it was observed that in samples V-5 and LL-3, in which relatively little plagioclase (except that present as albite rims) has been expelled, even small and poorly formed myrmekite occurrences such as that of Plate 6-B (from V-5) are very rare, whereas in TT-2 and LL-4 myrmekite occurrences such as that of Plates 7-A and 5-B are common.

Now, it is believed (Phillips, 1974) that calcium, which is truly dissolved in alkali feldspar must, owing to the crystal structure of alkali feldspar, be present as a

hypothetical compound often referred to (ibid) as Schwantke's molecule, which has the following formula:



As Equation 21 demonstrates, Schwantke's molecule, upon escaping from the alkali feldspar lattice would revert to anorthite, releasing quartz. A complete account of this mechanism for the generation of myrmekite is presented and defended in Phillips (1974). It is sufficient here that Equation 21 provides a plausible mechanism for the generation of myrmekite. The textural and other evidence presented in this study linking myrmekite to the expulsion of plagioclase argues circumstantially that some myrmekite occurrences can form through the breakdown of this persilicic anorthite component.

The present author envisages that myrmekite in the Old Chelsea outcrop formed in the following way. Under conditions of falling ambient temperature, as the high-temperature composition of the igneous alkali feldspar with respect to sodium and calcium became unstable as a single phase, plagioclase expulsion from the alkali feldspar crystals began. However the myrmekite formed under temperature conditions of the lower

amphibolite facies or higher, where albite is not stable. Under these relatively high-grade conditions the persilicic anorthite component of the expelled plagioclase (Schwantke's molecule) reacted with the albite component, releasing quartz, to form the existing myrmekitic andesine. As ambient temperature conditions shifted into the greenschist facies, any persilicic anorthite component would at this stage break down, presumably to saussurite and sericite, or to epidote. It is important that at least the preliminary stages of myrmekite formation must have occurred in conjunction with the exsolution of andesine within the alkali feldspar crystal. This exsolution process is also quartz-releasing, yet the microprobe analyses indicate that neither the exsolution lamellae nor the surrounding host are persilicic\*, which requires that the quartz released during exsolution was expelled from the crystals. Therefore, at least in the early stages of plagioclase expulsion, the albite and persilicic anorthite components of the present myrmekitic oligoclase must have reacted under conditions of excess ambient quartz. This ambient mobile quartz would have acted to retard escape

---

\* There are known occurrences of quartz occurring with plagioclase lamellae (Spencer, 1948, in Phillips, 1974) in alkali feldspar crystals.

Table 9: Old Chelsea Outcrop: Detailed Albite Modes

SAMPLE NO.	ALBITE RIMMING PLAG.	PLAG. LAMELLAE IN K-SPAR	K-SPAR	OTHERS	TOTAL POINTS COUNTED
TT-1	2.8	5.5	37.8	53.8	3000
TT-2(1)*	1.7	7.9	35.7	54.7	1374
TT-2(2)	2.2	2.7	25.0	70.2	637
TT-3(1)*	1.6	2.4	26.4	69.7	1148
TT-3(2)	0.8	1.0	15.7	82.5	1488
TT-3(3)	1.1	1.1	15.6	78.4	929
LR-1*	3.5	1.9	18.1	76.5	695
LR-2*	3.3	6.6	43.3	46.8	1737
LL-3*	1.9	10.7	51.8	35.7	900
LL-4(1)*	0.4	0.4	9.7	89.5	1339
LL-4(2)	2.1	5.2	33.4	59.3	2419
V-5(1)	2.3	3.4	32.0	63.1	1236
V-5(2)*	2.3	9.2	33.0	55.5	947

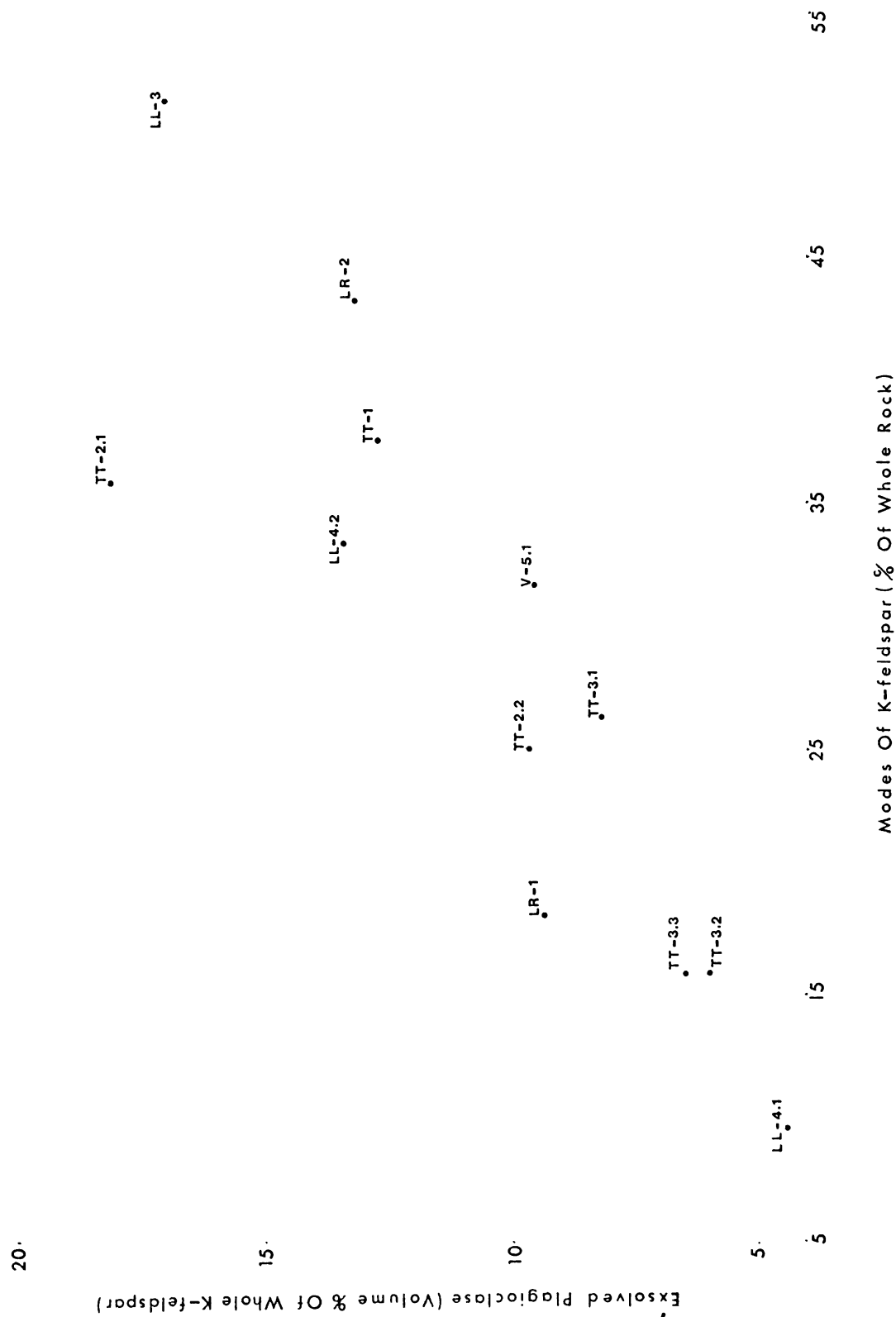
\* Microprobe target area

of the quartz liberated by Equation 21, abetting the formation of myrmekite.

The final stage in the understanding of the plagioclase expulsion process operant in the alkali feldspars of the Old Chelsea outcrop is an explanation of the variation in the extent to which plagioclase expulsion has occurred in the various study outcrop samples. Figure 13 provides at least a partial explanation. In Figure 13 are shown the results of the detailed point count studies of Table 9. On the ordinate is plotted the sum of the percentages of exsolved plagioclase expressed as a ratio of the percentage of perthitic alkali feldspar. On the ordinate is plotted the percentage of perthitic alkali feldspar. There is a distinct positive correlation between these two parameters: the more abundant is alkali feldspar in an area of the study outcrop, the more concentrated is the exsolved plagioclase within that alkali feldspar. The explanation for this phenomenon lies in the non-randomness of the alkali feldspar distribution in the study outcrop. In areas rich in alkali feldspar the mineral occurs in large aggregates which have impeded plagioclase expulsion by minimizing surface effects per unit volume. Also, from within the larger aggregates,

Figure 13: Modes of exsolved plagioclase lamellae in selected small areas of some Old Chelsea outcrop specimens with widely varying total alkali feldspar contents. Data were acquired from detailed point counts presented in Table 9.

Figure 13: Correlation Of Exsolved Plagioclase In K-feldspar To Modes Of K-feldspar  
V-5.2



521

(125)

the mobile plagioclase, plagioclase components, and quartz would have a longer distance to diffuse along grain boundaries and crystal defects to escape the alkali feldspar "clumps". This would act to retard the escape of the "unwelcome" plagioclase, creating a backlog in these high alkali feldspar areas.

## DISCUSSION

Geothermometry intimates that the alkali feldspar of the Old Chelsea outcrop crystallized from the primary magma in a disordered state and subsequently became ordered before or during the attainment of maximum metamorphic grade.

However, Stormer's (1975) two-feldspar geothermometer failed in two study areas to give consistent and geologically meaningful equilibration temperatures for the analysed feldspar pairs. Equilibrium between the plagioclase and alkali feldspar was very possibly present up to and at least partially including the time of exsolution of plagioclase in the alkali feldspar. However, this equilibrium, if ever present, has since been disrupted. Thus the failure of the Stormer geothermometer in this study is not provably attributable to any deficiency in the geothermometer itself, but is instead due to the disequilibrium between the feldspars analysed. Perhaps also culpable are the data themselves, for it is very difficult to analyse perthite with precision sufficient for geothermometry.

This study, then, has uncovered dangers in the

routine application of two-feldspar geothermometry to poly-deformed gneiss terrains, especially in those frequent cases where the alkali feldspar is perthitic. However, the study has failed to rigorously and fairly test Stormer's (1975) geothermometer, and the assumptions made in calibrating the geothermometer are neither affirmed nor disputed.

However, the study makes two contributions unrelated to practical field geothermometry. The first is a modified oil immersion technique which is much faster and more precise than the standard method.

Secondly, this study provides some insight into the mechanism operant during the disruption of equilibrium between plagioclase and alkali feldspar in the rocks studied. Plagioclase and its chemical components have been expelled from the alkali feldspar crystals of the Old Chelsea outcrop. Some crystals have expelled plagioclase in quantities exceeding 25 volume percent of the original crystals. The expulsion process was operant under conditions of falling ambient temperature, and especially near the rims of crystals, probably co-initiated with the exsolution of plagioclase from the alkali feldspar crystals. As well as the plagioclase

expelled by the diffusion of dissolved plagioclase components, some was expelled by bulk migration of exsolved plagioclase lamellae. The anorthite component of plagioclase, when dissolved in alkali feldspar, is believed to exist in a persilicic form known as Schwantke's molecule. Expelled Schwantke's molecule, near obvious zones of expulsion in the alkali feldspar crystals, reacted with expelled albite at temperatures above those of the greenschist facies to form myrmekitic andesine overgrowths on plagioclase crystals. At temperatures below those where andesine is stable, expelled plagioclase began to form an albite rim around plagioclase and around the myrmekite.

In samples rich in alkali feldspar, plagioclase expulsion was retarded by the large alkali feldspar aggregates in these samples. These aggregates reduced the relative amount of surface area of the crystals, and increased the distance which expelled plagioclase had to travel to escape the alkali feldspar crystals.

## SUGGESTED FURTHER RESEARCH

Some problems remain unanswered by the present study. Firstly, inhomogeneity in the host phase of the alkali feldspar studied is provable only in a rough, statistical way. Efforts in this direction were hampered by the choice of standard for the study, which being adularia, is not necessarily homogeneous at the microscopic level. Thus the experimental error determined by analysing the standard is a maximum figure, and the boundary between experimental error and demonstrable inhomogeneity in the unknowns is a fuzzy one. This problem can be overcome by preparing as standards several glasses of appropriate known composition (for example five, ten, and fifteen mole percent albite). With this done, the problem of microscopic-scale inhomogeneity can be attacked more powerfully. Also, more data could be amassed to compare the composition of zones of plagioclase expulsion to that of neighbouring areas.

On another front, the revised immersion oils technique presented herein is in need of a more rigorous calibration in properly warm surroundings. Following this, it should be tested on some pyroxenes or olivines of known composition.

Finally, it is possible that the processes of plagioclase expulsion from alkali feldspar crystals, and the ordering of aluminum and silicon within those crystals can operate simultaneously in response to falling temperature. Indeed, one process might well initiate the other. A study which directly sets out to discover the existence of this relationship would be of value, both to students of order/disorder, and to those of feldspar geothermometry.

## REFERENCES

- Barth, T. F. W. (1951): The Feldspar Geological Thermometers, *Neues Jahrb. Mineral.*, 82, pp. 143 - 154.
- Bohlen, S. R., and E. J. Essene (1977): Feldspar and Oxide Geothermometry of Granulites in the Adirondack Highlands, *Contrib. Mineral. Petrol.*, 62, pp. 153 - 169.
- Bourne, J. B. (1970): Geology of the Cayamant Lake Area: Preliminary Report, Quebec Dept. Na. Res. Prelim. Rept. P. R. - 598.
- Bowen, N. L. (1913): The Melting Phenomena of the Plagioclase Feldspars, *Am. J. Sci.*, ser 4, 35, pp. 577 - 599.
- Carmichael, I. S. E. (1967): The Iron-Titanium Oxides of Salic Volcanic Rocks and Their Associated Ferromagnesian Silicates, *Contrib. Mineral. Petrol.*, 14, pp. 36 - 64.
- Deer, W. A., R. A. Howie and J. Zussman (1966): "An Introduction to the Rock-Forming Minerals", Longman Group, London.
- Goldich, S. S., C. O. Ingemells, N. H. Suhr and D. H. Anderson (1967): Analyses of Silicate Rock and Mineral Standards, *Can. J. Earth Sci.*, 4, pp. 747 - 755.
- Hogarth, D. D. (1970): Geology of the Southern Part of Gatineau Park, National Capital Region, *Geol. Surv. Can. Geol. Rept.* 70-a.
- Johannsen, A. (1939): "Petrography", 2nd ed., Vol. 1, U of Chicago Press.
- Krauskopf, K. B. (1967): "Introduction to Geochemistry", McGraw-Hill, New York.
- Orville, P. M. (1972): Plagioclase Cation Exchange Equilibria With Aqueous Chloride Solution at 700° and 2000 Bars in the Presence of Quartz, *Am. J. Sci.*, 272, pp. 234 - 272.
- Parsons, I. (1978): Alkali-feldspars: Which Solvus?, *Phys. Chem. Minerals*, 2, no. 3, pp. 199 - 214.
- Phillips, E. R. (1974): Myrmekite - One Hundred Years Later, *Lithos*, 7, no. 3, pp. 181 - 194.
- Saxena, S. K., and P. H. Ribbe (1972): Activity-Composition Relations in Feldspars, *Contrib. Mineral. Petrol.*, 37 pp. 131 - 138.

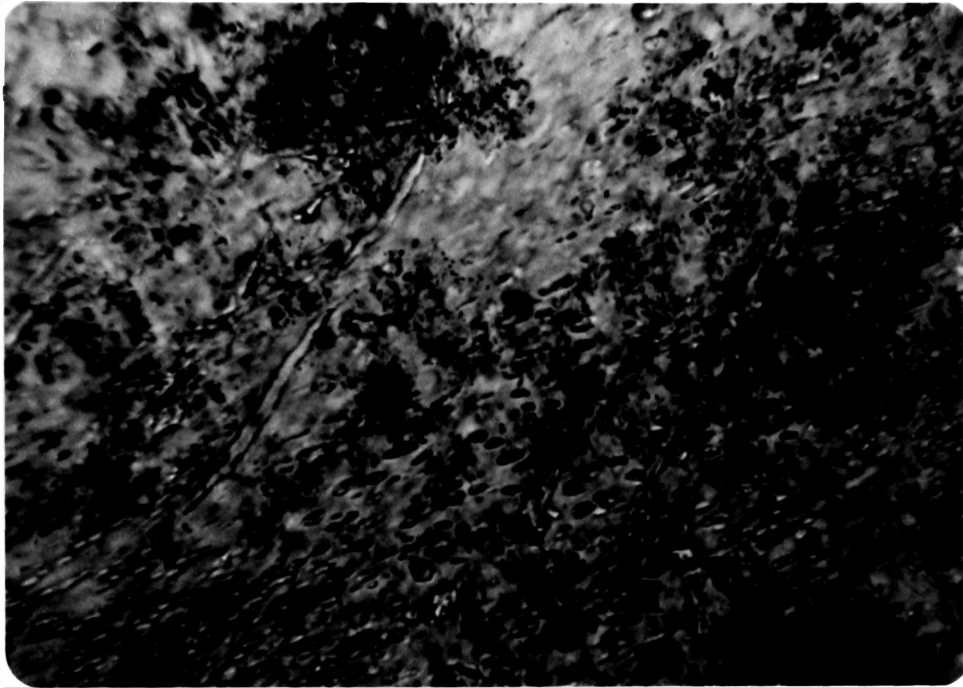
- Seck, H. A. (1971): Der Einfluss des Drucks auf die Zusammensetzung Koexistierender Alkali Feldspate und Plagioclase in System  $\text{NaAlSi}_3\text{O}_8 - \text{KAlSi}_3\text{O}_8 - \text{CaAl}_2\text{Si}_2\text{O}_8 - \text{H}_2\text{O}$ , Contrib. Mineral. Petrol., 31, pp. 67 - 86.
- Smith, Joseph V. (1974): "Feldspar Minerals: Chemical and Textural Properties", Vol. 2, Springer-Verlag, New York. Heidelberg. Berlin.
- Stewart, J. B. (1974): Optic Axial Angle and Extinction Angles of Alkali Feldspars Related by Cell Parameters to Al/Si Order and Composition, In: (W. S. MacKenzie and J. Zussman, eds.), "The Feldspars", pp. 145 - 161.
- Stormer, J. C. (1975): A Practical Two-Feldspar Geothermometer, Am. Mineral., 60, pp. 667 - 674.
- \_\_\_\_\_ (1976): Geothermometry and Geobarometry in Epizonal Granitic Intrusions: A Comparison of Iron-Titanium Oxides and Coexisting Feldspars, Am. Mineral., 61, pp. 751 - 761.
- Streckeisen, A. (1967): Classification and Nomenclature of Igneous Rocks, Neues. Jahrb. Mineral. Abhandl., 107, pp. 144 - 240.
- Thompson, J. B., and D. R. Waldbaum (1969a): Mixing Properties of Sanadine Crystalline Solutions: III. Calculations Based on Two-Phase Data, Am. Mineral., 54, pp. 811 - 838.
- \_\_\_\_\_ and \_\_\_\_\_ (1969b): Mixing Properties of Sanadine Crystalline Solutions: IV. Phase Diagrams from Equations of State, Am. Mineral., 54, pp. 1274 - 1298.
- Whitney, J. A., and J. C. Stormer (1977a): Two Feldspar Geothermometry and Geobarometry in Mezozonal Granite Intrusions: Three Examples from the Piedmont of Georgia, Contrib. Mineral. Petrol., 63, no. 1, 1977, pp. 51 - 64.

- \_\_\_\_\_ and \_\_\_\_\_ (1977b): The Distribution of  $\text{NaAlSi}_3\text{O}_8$   
Between Coexisting Microcline and Plagioclase and  
its Effect on Geothermometric Calculations, Am.  
Mineral., 62, pp. 687 - 691.
- Wynne-Edwards, H. R. (1969): Tectonic Overprinting in  
the Grenville Province, Geol. Assoc. Can. Sp. Pap.  
no. 5.

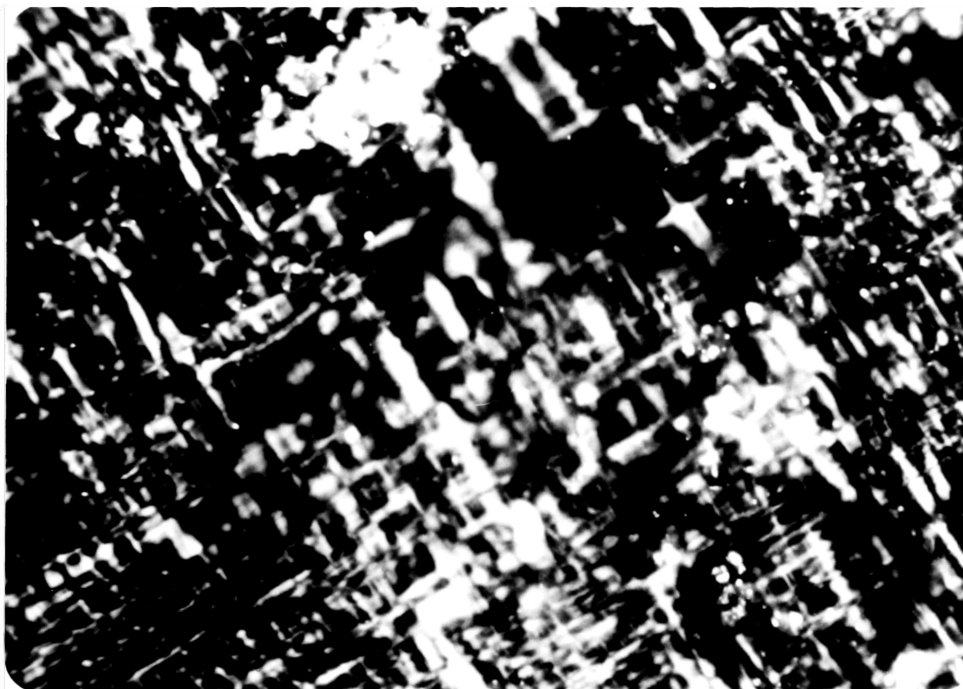
Plate 1

A: LL-3; magnification - 200X; crossed polars. The alkali feldspar target crystal, in the vicinity of microprobe analysis PC-83. Note the coarseness of some plagioclase lamellae (high-relief blebs) contrasting with the swarms of consistently oriented, much finer lamellae nearby.

B: LL-3; magnification - 80X; crossed polars. The same location as Plate 1-A. Note that the large plagioclase crystal (top left) is rimmed by albite and is myrmekitic (top center) where it adjoins the vague zone of coarse plagioclase lamellae including that of PC-83.

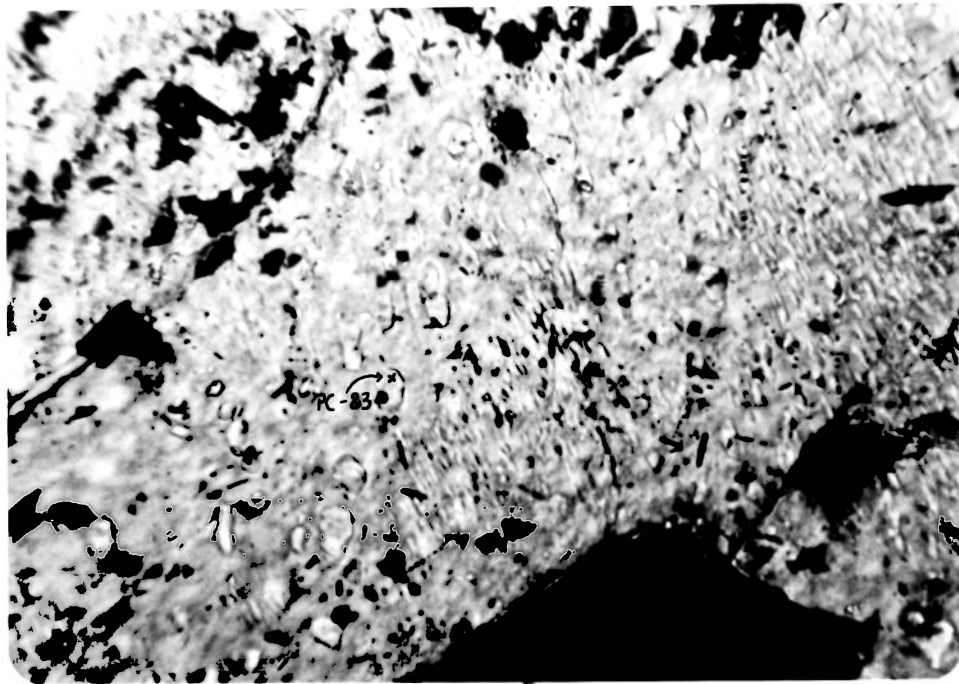


2-A



2-B

PLATE 2



0.10 mm

1-A



0.25 mm

1-B

PLATE 1

Plate 2

A: TT-1; magnification - 200X; plain light. A portion of an alkali feldspar crystal showing inhomogeneity in distribution of exsolved plagioclase lamellae. Note in particular the plagioclase-poor area (top center) to right of the dark patch of sericite. Note as well, the elongate ribbons of exsolved plagioclase just left of center, and how they curve into an area (lower left) where small equant blebs are coalescing into larger more elongate lamellae.

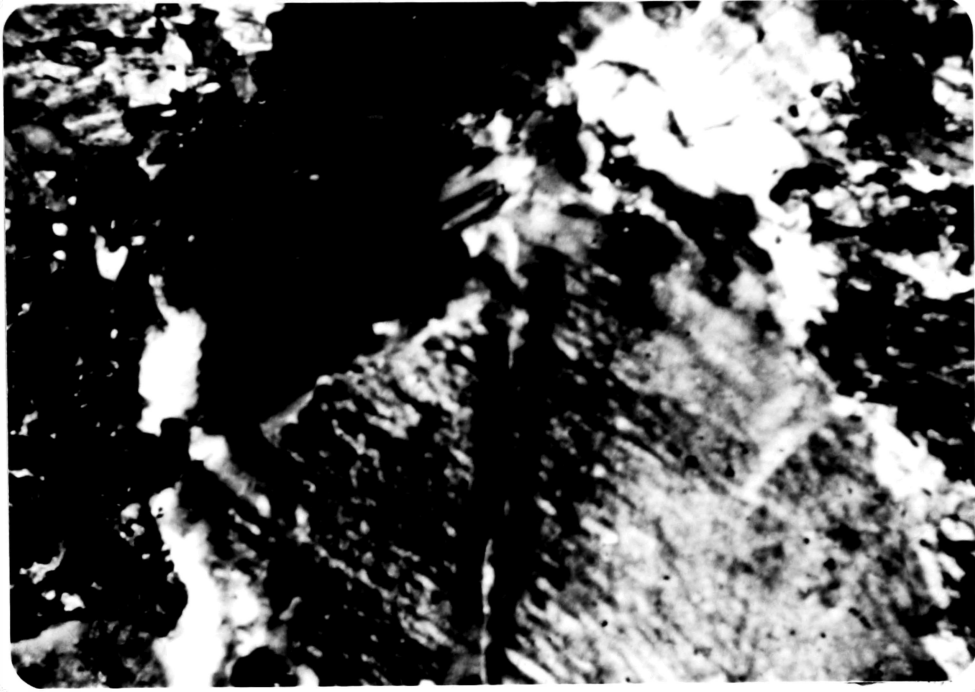
B: TT-1; magnification - 200X; crossed polars. The same location as Plate 2-A. Note the diffuseness of patchwork twinning in the plagioclase-poor area, as compared to the surrounding, more densely perthitic areas.

Plate 3

A: V-1; magnification - 80X; crossed polars. Blocky exsolved alkali feldspar in a lath-like, albite rimmed plagioclase crystal.

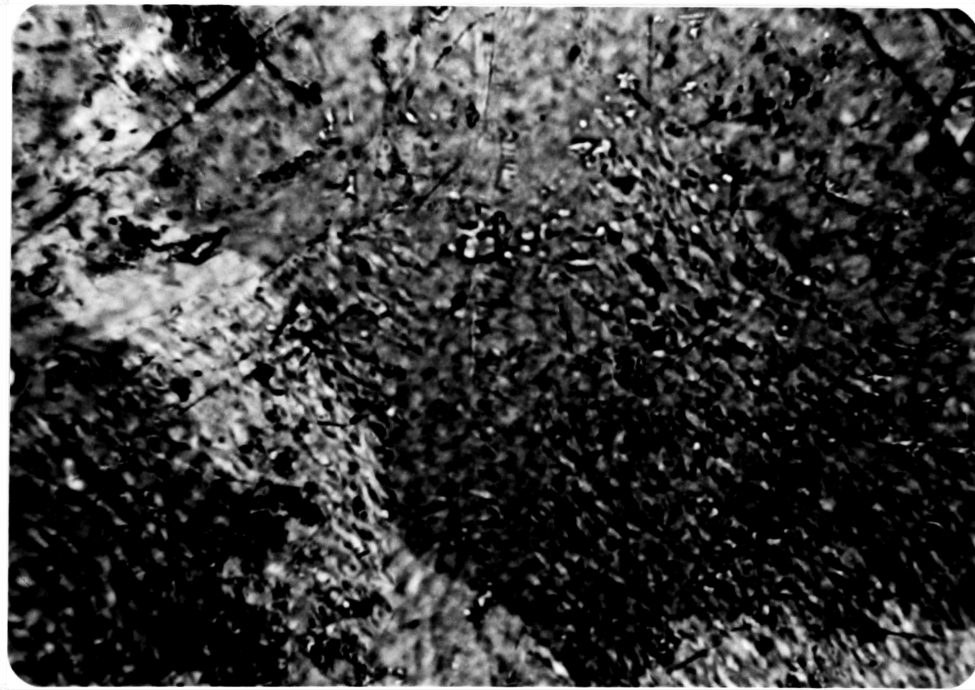
B: V-6 Station no. 1; magnification - 80X; crossed polars. The alkali feldspar target crystal and the sites of microprobe analyses KF-121 and -122. Those are taken from a plagioclase-free, untwinned zone. Note the abundance of nearby albite (higher birefringence) rimming the neighbouring plagioclase crystal and within the alkali feldspar crystal itself.

0.25 mm



4-A

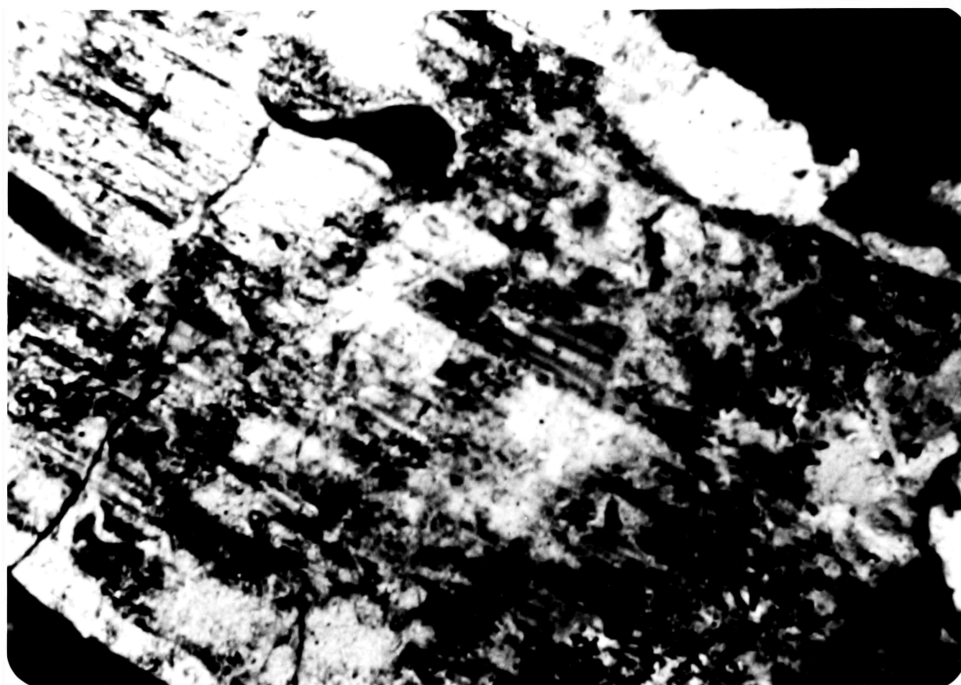
0.10 mm



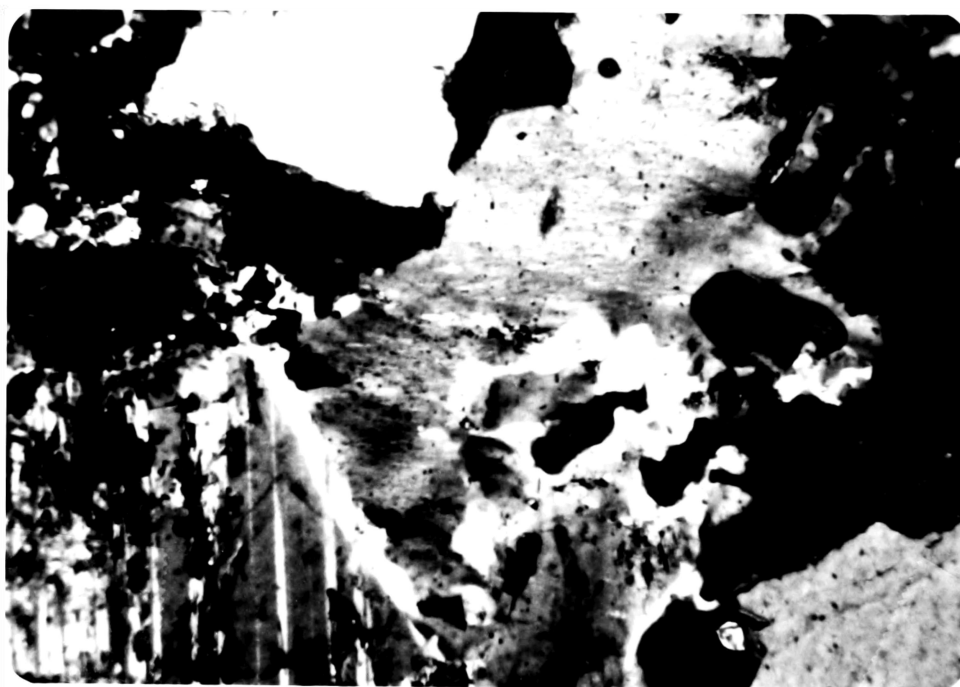
4-B

PLATE 4

(138)



3-A



3-B

PLATE 3

Plate 4

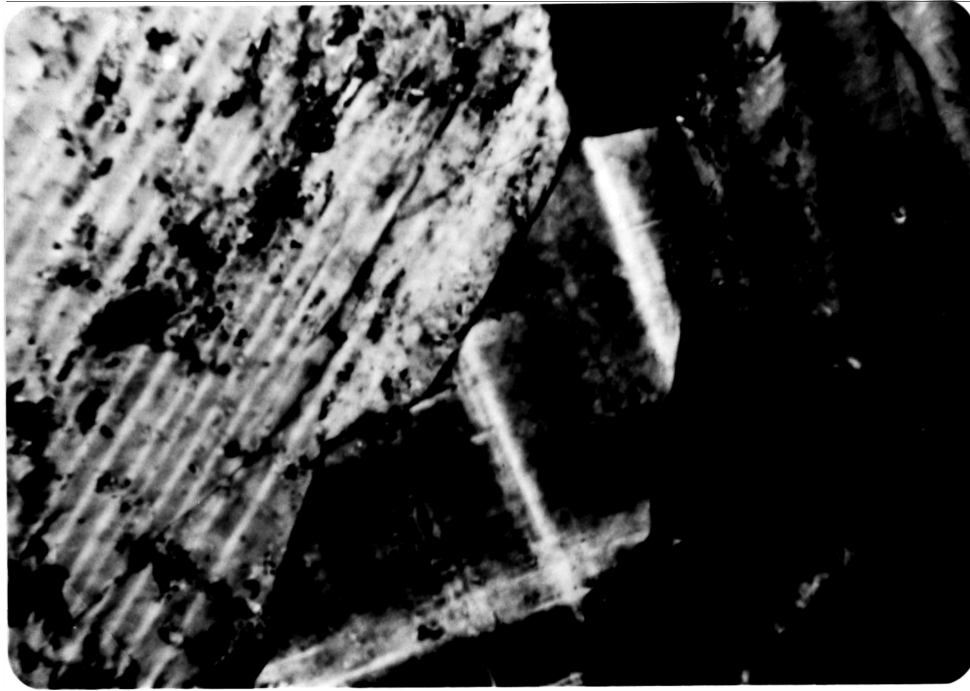
A: LR-1; magnification - 80X; crossed polars. A plagioclase-free band around a crack in an alkali feldspar crystal. The band is demarcated by the diffuseness of twinning within it. Note the thick albite rim on the neighbouring plagioclase crystal (at extinction) where it adjoins the plagioclase-free band.

B: LR-1; magnification - 200X; plain light. A close-up of the plagioclase-free band described in Plate 4-A. The crack in the crystal is occupied by elongate plagioclase lamellae.

Plate 5

A: LL-2; magnification - 200X; crossed polars. A small alkali feldspar crystal in which albite expulsion has proceeded nearly to completion. Again, the twinning is diffuse. Atypically, albite and myrmekite are not developed on the surrounding plagioclase.

B: TT-2; magnification - 80X; crossed polars. Myrmekitic excrescences on plagioclase crystals. Note in particular the large protrusion at centre. Extinction here is almost simultaneous with that of the adjoining plagioclase crystal (bottom center). Note as well that the myrmekite is not separated from the plagioclase crystal by a distinct grain boundary, but by an almost invisible "weld".

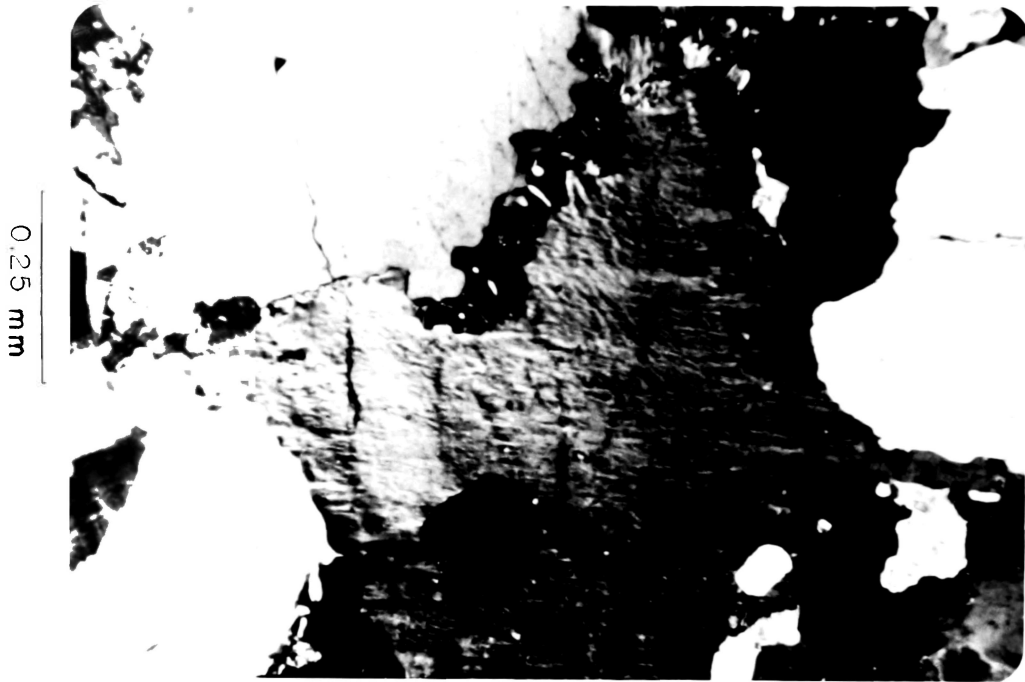


5-A

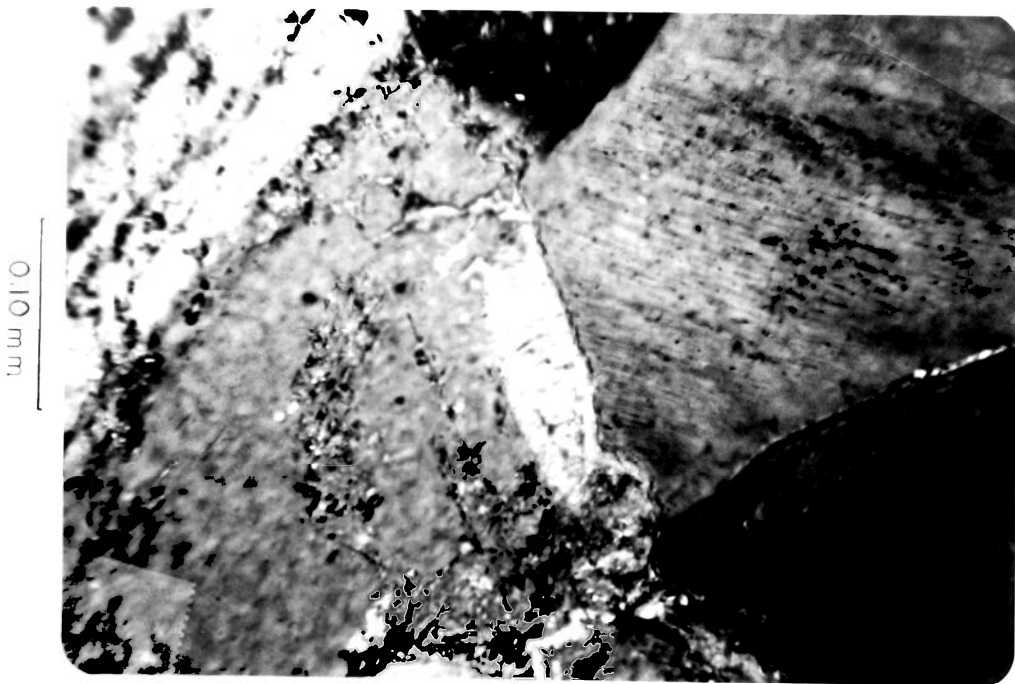


5-B

PLATE 5



6-A



6-B

PLATE 6

(140)

Plate 6

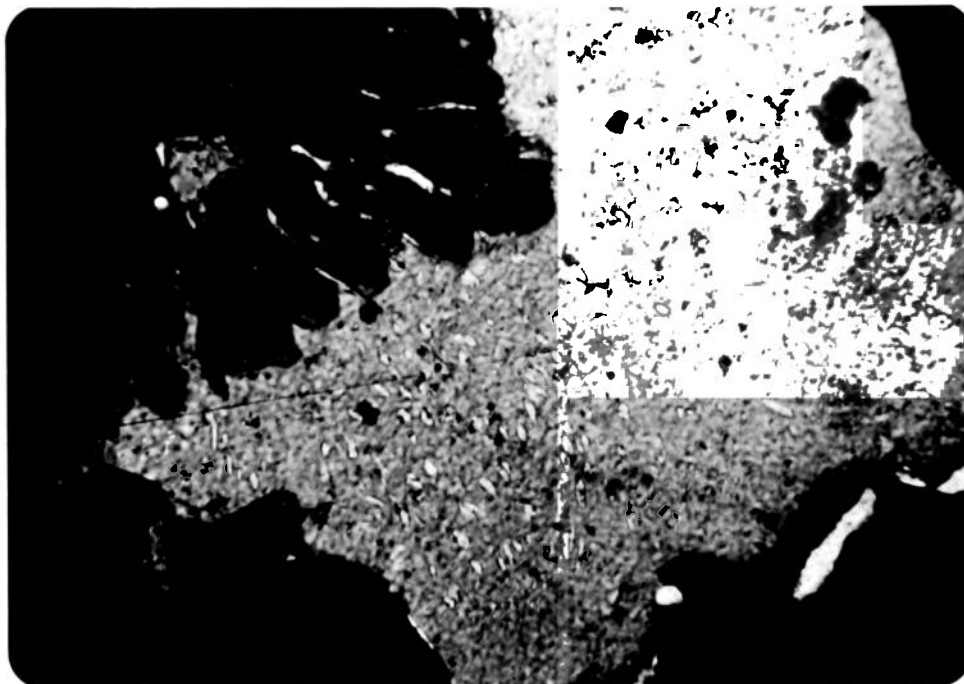
A: TT-2; magnification - 80X; crossed polars. An irregular myrmekitic plagioclase grain (just above center) between quartz and alkali feldspar. Note how, near the myrmekite the exsolved plagioclase lamellae in the alkali feldspar depart from their normal crystallographically controlled orientation in the crystal (horizontal in this photograph) and "stream in" to the myrmekite. Note also the vague, roughly conical area in the alkali feldspar crystal adjoining the myrmekite (just below and to the right of center) in which birefringence is apparently slightly higher. This results from a slightly rotated extinction position in the conical area, as compared to other parts of the crystal.

B: V-5; magnification - 200X; crossed polars. A small, poorly-formed occurrence of myrmekite.

Plate 7

A: TT-2; magnification - 80X; crossed polars. Large, sparse, disoriented plagioclase lamellae in an alkali feldspar crystal. Note the abundance of nearby myrmekite.

B: TT-2; magnification - 80X; crossed polars. Zone of "disturbed" exsolved plagioclase lamellae in alkali feldspar. The normal orientation is shown at right. Note that at the lower left the lamellae themselves bend into the zone of disturbance.



7-A



7-B

PLATE 7

(141)